Development of a Biosensor for Detection of Cancer Biomarkers

Ana Elisa Alves Silva

Master of Chemistry

Chemistry and Biochemistry Department

2020

Supervisor

Prof. Dr. Carlos Manuel de Melo Pereira, Faculty of Sciences of the University of Porto

Co-Supervisor

Dr. José Ribeiro, Faculty of Sciences of the University of Porto

U.PORTO

FACULDADE DE CIÊNCIAS
UNIVERSIDADE DO PORTO

Todas as correções determinadas pelo júri, e só essas, foram efetuadas.

O Presidente do Júri,

Porto, _____/_____/_____

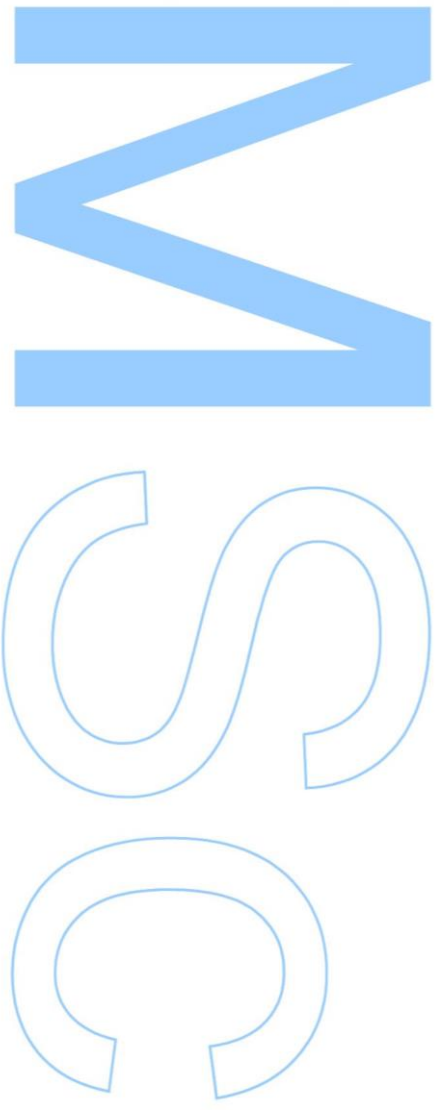

Acknowledgements

Throughout this year of learning and hard work, numerous people contributed so that this thesis came to fruition. I firstly thank my supervisor, Professor Carlos Pereira, for the chance to work on this project and all the support given to me. I would also like to thank my co-supervisor, Doctor José Ribeiro, for all the patience and support given, as well as all the advice, knowledge, and time. Without his help, it wouldn't have been possible to finish this project. I thank him as well for all the help at the SPR analysis. From both my supervisor and co-supervisor I have to thank the opportunity of letting me contact with what research is, with all its success. Thank you for showing me that effort and good work is always rewarded, and for leaving me curious and craving for more.

My sincere thanks go also to all the docents, researchers and colleagues from the Centro de Investigação em Química da Universidade do Porto (CIQUP), specially to Renata Costa, Tânia Rebelo, Ana Brandão, Thacilla Menezes, Paula Fernandes, Patrícia Moreira and Natália Sousa for all the sympathy, help and scientific discussions, as well as all the good work environment.

On a personal note, I would like to firstly thank my friends, specially to Ana Sofia Silva, Andreia Guimarães, Rita Sousa, Mário Pinho, Ricardo Melo, Sofia Pires, Alexandra Silva, Pâmela Guimarães, Catarina Henriques, and Ana Costa, among others, for the company and care on the last few years.

To my childhood friends, Rita Oliveira, Catarina Gomes, and Inês Ribeiro thank you for always being by my side after so many years, and for believing in me.

I finally thank my family, especially my grandparents, Diamantino and Hermínia "Minuxa", and my parents, José e Ana Luísa. Despite all the distance, you always had a word of advice and energy to make me go on another day in this hard path. To my little sister, Nor, for being my biggest support and always believing in me. For all the video calls when days were rough, and all the smiles you provided. To my godfather, for all the advice when times were tough. To you all, I dedicate this thesis, for all the immense effort made, all the dedication, and for always believing in me, even when I didn't.

Resumo

Este trabalho teve como objetivo o desenvolvimento de um novo biossensor eletroquímico, tendo como base a impressão molecular para a deteção seletiva de biomarcadores de cancro, no ponto de cuidado.

Elétrodos impressos de ouro (AuSPEs) foram usados como transdutores, visto que o seu pequeno tamanho (portabilidade), descartabilidade e baixo custo de produção permitem a aplicação em contexto de diagnóstico clínico.

A preparação das superfícies sensores englobou os seguintes passos: primeiramente, a deposição de uma monocamada automontada (SAM) no elétrodo de trabalho permitiu a imobilização de proteína alvo na superfície do elétrodo. A albumina de soro bovino (BSA) foi utilizada como *template* nos estudos de otimização. Seguidamente, as cavidades específicas do polímero molecularmente impresso (MIP) foram criadas através da eletropolimerização, utilizando a técnica de voltametria cíclica (CV) do 3-aminofenol (monómero), na presença do *template*, originando um filme polímero, o poli(3-aminofenol), contendo a molécula alvo. Finalmente, após a remoção do *template* da matriz polimérica, o MIP foi capaz de reconhecer e ligar-se de forma seletiva às proteínas usadas como *template*.

A modificação da superfície dos *chips* foi monitorizada através de medições eletroquímicas, utilizando as técnicas de voltametria cíclica (CV) e de voltametria de onda quadrada (SWV), na presença do par redox hexacianoferrato(III)/hexacianoferrato(II). A performance do biossensor foi avaliada utilizando SWV como técnica analítica.

Na primeira parte deste trabalho, as condições experimentais para a preparação das superfícies de detenção foram otimizadas, através de: (i) estudo da sonda redox mais apropriada tendo como base a superfície do elétrodo impresso de ouro (AuSPE), (ii) seleção de uma SAM, com propriedades hidrofóbicas (hexano-1-tiol, HT) ou hidrofílicas (8-amino-octano-1-tiol, AOT) para imobilização eficaz da proteína alvo, antes do processo de eletropolimerização, de forma a evitar desnaturação da proteína; (iii) otimização das condições experimentais para a eletropolimerização do monómero e controlo da espessura do filme (através do controlo do número de ciclos realizados durante a CV a uma velocidade de varrimento predefinida) de modo a aumentar a performance do biossensor; (iv) seleção de um método eficiente de extração de proteína alvo da matriz polimérica.

Na segunda parte do trabalho, a performance do biossensor preparado foi avaliada através da realização de estudos de detenção que consistiram na incubação da superfície do sensor com soluções com concentração crescente do analito, de forma a construir as curvas de calibração (e estimar o intervalo de resposta linear, sensibilidade e limite de detenção). Os ensaios foram reproduzidos tendo como sistema de o polímero não-impresso (NIP).

Resumidamente, a detenção da BSA foi realizada através da imobilização da proteína alvo numa SAM de AOT, seguida de eletropolimerização do monómero 3-aminofenol usando apenas um (ou dois) ciclos durante a CV de forma a obter filmes ultrafinos na superfície do elétrodo. De seguida, a proteína modelo foi removida da matriz polimérica através da incubação do *chip* com uma solução de dodecil sulfato de sódio (SDS). Após a realização dos estudos de detenção da BSA, os resultados obtidos mostram que a adsorção não-específica apresenta uma contribuição relevante durante o processo de ligação e estratégias para reduzir este fenómeno são descritas. Finalmente, o conhecimento adquirido durante o trabalho realizado iria ser aplicado para a deteção de biomarcadores de cancro, usando a mesma estratégia de impressão molecular.

Palavras-Chave

Polímero molecularmente impresso; biomarcador de cancro; AuSPE; ponto de cuidado; biossensor eletroquímico; eletropolimerização; voltametria cíclica; voltametria de onda quadrada; hexacianoferrato(III)/hexacianoferrato(II).

Abstract

The main objective of this work was to develop a new electrochemical biosensor device, based on molecularly imprinting (MI) technology for detection of cancer biomarkers, in point-of-care (PoC). Gold screen-printed electrodes (AuSPEs) were used as transducers, since their small size (portability), disposability and low production cost allows their application in clinical diagnosis context.

The overall fabrication process incorporated the following steps: first, the deposition of a self-assembled monolayer (SAM) on the electrode working area allowed the immobilization of the target protein at the electrode surface. Bovine serum albumin (BSA) was used template in these optimization studies. Then, the specific binding sites were created by cyclic voltammetry (CV) electropolymerization of 3-aminophenol monomer, in the presence of the template protein, giving origin to a non-conductive poly(3-aminophenol) thin film containing the template biomolecules physically entrapped. Finally, target biomolecules were removed from the polymeric matrix and the resulting MIP film was able to recognize and selectively binds to template molecules during the rebinding studies.

The evaluation of surface chemical modification procedures was achieved by performing electrochemical measurements, using cyclic voltammetry (CV) and square wave voltammetry (SWV), in the presence of the well-characterized ferrocyanide/ferricyanide reporting system. The MIP receptor detection performance was evaluated by using SWV as analytical technique.

In the first part of this work, the experimental conditions for preparation of the biosensing surfaces were optimized, namely: (i) study of the appropriate redox probe as reporting system; (ii) selection of a suitable SAM, having hydrophobic (hexane-1-thiol, HT) or hydrophilic (8-amino-octane-1-thiol, AOT) properties, for effective immobilization of the target protein at the electrode, prior to electropolymerization process, in order to avoid protein denaturation; (iii) optimization of the experimental conditions for monomer electropolymerization and control of film thickness (by controlling the number CV cycles at a defined scan rate) to improve detection performance; (iv) selection of an effective method for protein extraction from the polymeric matrix.

In the second part of this work, the performance of the prepared MIP-based biosensor was evaluated by performing protein rebinding studies, consisting in the incubation of the sensor surface with solutions with increasing concentration of analyte in order to build the calibration curves (and estimate linear response range, sensitivity

and LOD). The experiments were performed in parallel using the non-imprinted polymer (NIP) as reference system.

In brief, best preliminary results for detection of BSA were achieved by immobilizing the target protein on an AOT SAM, following by CV electropolymerization of 3-aminophenol monomer using one (or two) CV cycle in order to obtain thin MIP films at the chip surface. After that, the template protein was washed out by incubating the electrode surface with a solution containing sodium dodecyl sulphate (SDS). After performing the detection studies, the preliminary results obtained show that non-specific interactions had a relevant contribution during the rebinding process and strategies to reduce the non-specific adsorption are described. Finally, the know-how acquired from the work performed should be transposed for the detection of cancer biomarkers using the same MI strategy.

Key-words

Molecularly imprinted polymer; cancer biomarker; AuSPE; point-of-care, electrochemical biosensor; electropolymerization; cyclic voltammetry; square wave voltammetry; ferrocyanide/ferricyanide.

Contents

List of Figures

List of Tables

List of Equations

Symbols and Acronyms

A – Area of the electrode

ABS – Acetate buffer solution

AOT – 8-Amino-octane-1-thiol

APh – 3-Aminophenol

AuSPE – Gold screen-printed electrode

BSA – Bovine serum albumin

c – Specie bulk concentration

c_0 – Concentration of species

CA 15-3 – Carbohydrate antigen 15-3

CV – Cyclic voltammetry

D – Diffusion coefficient

DMSO – Dimethyl sulfoxide

DPV – Differential pulse voltammetry

$E^{0'}$ – Species formal potential

ELISA – Enzyme-linked immunosorbent assay

EP – Electropolymerization

E_{pa} – Cyclic voltammetry anodic peak potential

E_{pc} – Cyclic voltammetry cathodic peak potential

eSPR - Electrochemistry combined-surface plasmon resonance

E_{start} – Cyclic voltammetry initial potential

E_{λ} – Cyclic voltammetry switching potential

F – Faraday constant

f – Square wave voltammetry frequency

FDM – Ferrocenedimethanol

HAR – Hexaammineruthenium

HER2-ECD – Human epidermal growth factor receptor 2

HT – Hexane-1-thiol

I_F – Square wave voltammetry forward peak current intensity

$I_{p,a}$ – Cyclic voltammetry anodic peak current intensity

$I_{p,c}$ – Cyclic voltammetry cathodic peak current intensity

$I_{peak(SWV)}$ - Square wave voltammetry peak current intensity

I_R – Square wave voltammetry reverse peak current intensity

IUPAC – International Union of Pure and Applied Chemistry

LOD – Limit of detection

MCH – 6-Sulfhydryl-hexane-1-ol (also known as 6-mercapto-hexane-1-ol)

MI – Molecular imprinting

MIP – Molecularly imprinted polymer

n – Number of electrons

NIP – Non imprinted polymer

p.a. – practical grade

PBS – Phosphate buffer solution

PoC – Point-of-care

PSA – Prostate specific antigen

RSD - Relative standard deviation

SAM – Self-assembled monolayer

SDS – Sodium dodecyl sulphate

SPE – Screen-printed electrode

SPR - Surface plasmon resonance

SWV – Square wave voltammetry

ΔE_p – Square wave voltammetry pulse amplitude potential

ΔE_s – Square wave voltammetry step potential

ζ – Dimensionless electrode potential

τ – Square wave voltammetry period

ν – Cyclic voltammetry scan rate

1. Introduction

1.1. Objectives

1.2. Biosensors

1.2.1. Recognitions Elements

1.2.1.1. Molecularly Imprinted Polymers

1.2.2. Electrochemical Transducers

1.2.2.1. Screen-printed Electrodes

1.3. State of the Art

1.4. Techniques of Surface Characterization

1.4.1. Electrochemical Techniques

1.4.1.1. Cyclic Voltammetry

1.4.1.2. Square Wave Voltammetry

1. Introduction

1.1. Objectives

The main goal of the present work was the development of a new molecularly imprinted polymer-based electrochemical device for detection of cancer biomarkers in point-of-care (PoC). The specific binding sites were prepared by electropolymerization (EP) of the selected monomer, 3-aminophenol, on gold screen-printed electrodes (AuSPE) substrates, in the presence of the protein biomarker template, followed by extraction from the polymeric matrix.

The main innovation of the biosensor prepared was the use of thiol based self-assembled monolayers (SAMs) for the protein immobilization, which provides a stable base for the protein immobilization without occurring denaturation.

In preliminary studies for optimization of the molecularly imprinted polymers (MIP) synthesis procedures, BSA was selected as template protein. This molecule is well studied and was already used as template in preparation of MIP-based biosensors [1]. Bovine serum albumin (BSA) is a relatively small globular protein, with a molecular weight of 66.5 kDa, and presents an isoelectric point between pH 4.5 and 5.0, being negatively charged at physiological pH. The main advantages associated to the use of this molecule are its high stability and water solubility. After these preliminary studies, the know-how acquired was meant to be transposed for the preparation of a MIP-based biosensor for screening prostate specific antigen (PSA), a prostate cancer biomarker of similar size to BSA.

The biosensor preparation was followed step-by-step using voltammetric techniques, namely Cyclic voltammetry (CV) and square wave voltammetry (SWV), in the presence of a ferrocyanide/ferricyanide redox probe. For the quantification studies SWV technique was used.

1.2. Biosensors

A biosensor is a type of chemical sensor that uses a biochemical mechanism to transform molecular information into a physico-chemical output signal [2, 3]. Briefly, a biorecognition system allows the molecular information to be transformed into a measurable signal, providing it with a high degree of sensitivity, while the transducer converts the signal originated on the recognition system into analytical information [2, 3] (see Fig. 1). The molecular information is based on the detection of the complex

between the biorecognition element and the analyte, such as enzyme-substrate and antigen-antibody complexes [3]. After the reaction between the recognition element and the analyte takes place, the transducer transforms the collected information into a measurable signal, capable of being displayed and analysed [3].

Biosensors can be classified based on both the nature of the receptor system used and the transducer system, as shown in Fig. 1.1.

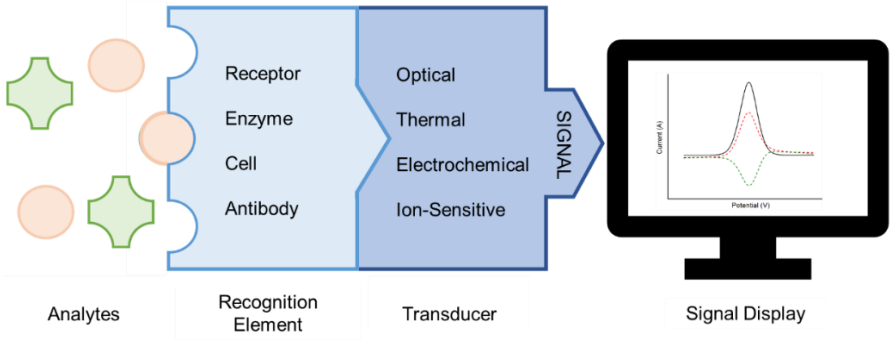

Figure 1.1 – Schematic representation of a biosensor structure – adapted from reference [3]

1.2.1. Recognition Elements

The recognition element is the component of the biosensor responsible for the selective interaction with the analyte [3].

With the advance of technology, different types of recognition elements have been used in biosensors, and its recognition system can be based in two processes, namely, biocatalytic or bioaffinity interactions [3]. The first recognition system focus on the recognition of reactions catalysed by biomolecules, and normally use enzymes, cells or tissues while bioaffinity systems recognize the interations between the analyte and macromolecules used as receptor systems, such as interactions occuring between an antigen and an antibody [3].

Despite the success on the recognition of analytes using biomolecules such as antibodies, various issues related to the stability and maintenance of the biomolecules have been described, such as low shelf-time, restricted temperature and pH conditions of preservation, reactivity with other chemicals, low abundance and high costs. Thus, the biosensors that employ these biomolecules as recognition system can suffer from lack of sensitivity, instability and low reproducibility [4, 5].

To overcome these limitations, an appealing solution consisted on the creation of biomimetic artificial receptors through the molecular imprinting of synthetic polymers (plastic antibodies) [4].

1.2.1.1. Molecularly Imprinted Polymers

Molecular imprinting (MI) is a process based on the lock and key mechanism. The preparation of this synthetic matrices is based on three main steps that can be seen in Fig. 1.2. Before polymerization, the monomer interact through covalent and/or non-covalent interactions (see Fig. 1.2a-b), followed by polymerization of the monomer (see Fig. 1.2c) and posterior removal of the target molecule from the polymeric matrix (see Fig. 1.2d) [6-8]. After the removal of the template, cavities complementary to the target molecule, known as binding sites, are left in the molecularly imprinted polymer (MIP) [6-8].

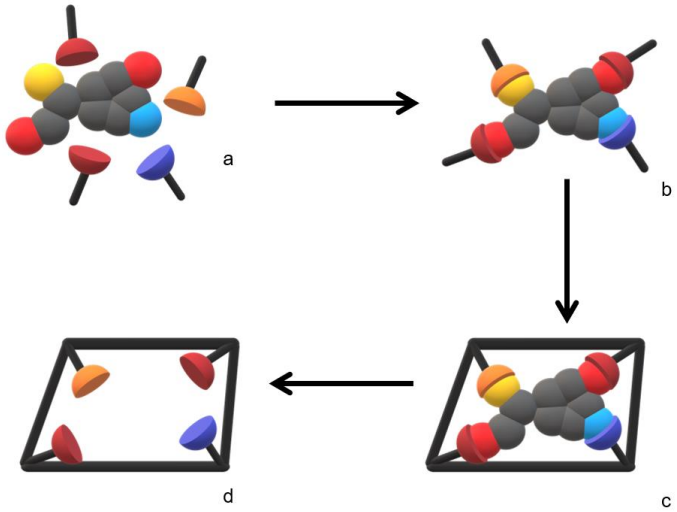

Figure 1.2 - Generical process of creation of a MIP (a-b) Interaction between monomers and template. (c) Polymerization. (d) Removal of the template. Adapted from reference [8]

Bulk preparation methods of MIPs are based on the polymerization of the monomer in the presence of a template molecule in order to imprint it in its polymeric matrix [9, 10]. However, this process only presents advantages when applied to small target molecules, since its removal from the polymeric matrix is rather easy, fast, and reversible. When bulk preparation is applied to large molecules, such as proteins, major problems related to difficulties in removing the biomolecules from the bulk of the matrix can compromise the extraction procedure, resulting in biosensors with long response or even no response to the binding of the protein due lack of binding sites [10]. Besides, issues related to template instability when the polymerization occurs under non-physiological conditions and low reproducibility of the preparation of MIP sensor platforms and have been described in literature [10].

In recent years, MIPs prepared by electropolymerization (EP) has become a very promising approach in the biosensors field [11-13]. This preparation procedure is based on the deposition of polymers, having conductive or non-conductive properties, on an electrode surface by using electrochemical techniques, such as CV or chronoamperometry [9], and it presents the advantages of simple and fast polymerization procedures without the need of using reaction initiators, and strong adhesion of the film to the transducer surface (stability) [7, 14]. Also, the easy control of the parameters of electrochemical techniques during the electropolymerization of the monomer, namely the number of cycles on CV or the time of applied potential in chronoamperometry, gives the possibility of easy control the film thickness and morphology by changing the amount of charge that flows through the system at the moment of polymerization [14].

After the electropolymerization occurs in the presence of the template molecule an effective washing procedure is mandatory for creation of the specific binding sites. Several protein extraction procedures have been described in the literature. Most of the protocols are based on biological agents, such as enzymes (trypsin [11], proteinase K [15]), or chemical solutions, such as acidic (acetic acid [13]) and basic (sodium hydroxide [12]) solution, containing or not additives, such as surfactants (e.g., SDS [13]).

A less explored issue when preparing MIPs for large biomolecules is the immobilization (or not) of the template prior to electropolymerization. According to the literature [7], three main procedures can be used for the electrosynthesis of MIPs, namely:

(i) simple electropolymerization of a solution containing both, target molecule and monomer. This approach has the advantage of being very simple, however, irreversible adsorption and/or denaturation of proteins on gold electrode surface has been described for bovine [16] and human [17] serum albumin, affecting the imprinting process.

(ii) adsorption of the target molecule on the electrode surface prior to the electropolymerization using a pure monomer solution (without template protein). Although it is a simple method, it also has the disadvantages of the previously described approach.

(iii) covalent (oriented binding) or non-covalent immobilization of the target molecule to structures deposited on the transducer, such as self-assembled monolayers (SAMs) [7, 9], prior to the electropolymerization. This approach has the advantage of formation of more uniform binding sites in the MIPs but

for proteins covalently immobilized the extraction of protein can be rather difficult and time-consuming.

In this work we used alkanethiols for assembly of a SAM on top of a gold substrate, for the non-covalent immobilization of template protein, allowing an effective and reversible removal of the protein from the MIP, that would not be possible using covalent immobilization methods [9, 18, 19], and avoid protein denaturation during the imprinting due to the strong hydrophobic interaction with the gold surface (see Fig. 1.3). Besides, SAMS allow the formation of a stable and well-defined organic film surface, due to the high affinity between the sulfur atom from the thiol functional group and the gold substrate [18, 19].

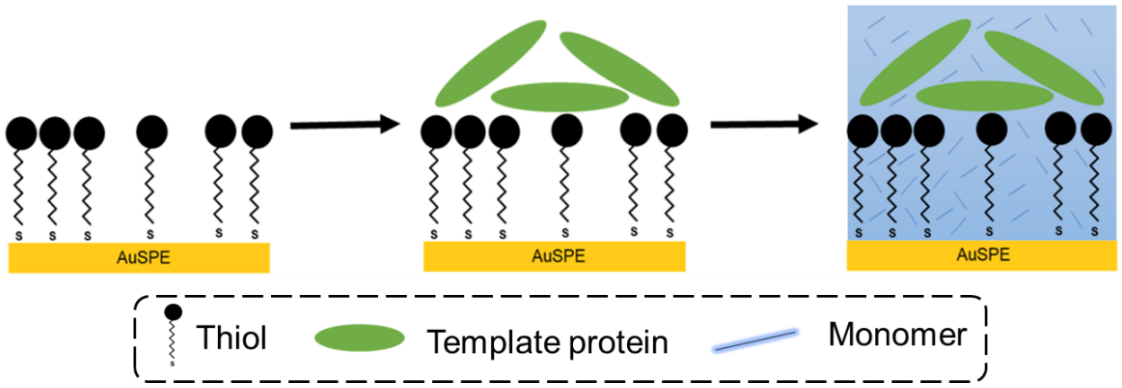

Figure 1.3 - Immobilization of a template protein on a pre-formed SAM deposited on an electrochemical transducer (AuSPE).

1.2.2. Electrochemical transducers

The main techniques used in for detection on electrochemical biosensors are (i) amperometric and voltammetric techniques, that rely on the measurement of electric current in the system, such as cyclic voltammetry and chronoamperometry; (ii) potentiometric techniques, that measure the voltage in the system and; (iii) conductometric techniques, that measure the conductivity or resistivity of the system [20].

As stated before, electrochemical sensors have been used for detection of several important chemical and biological biomolecules, including disease biomarkers [7, 11-13, 21, 22]. One common and simple approach to detect these biomolecules is by monitoring the permeability of a selected redox marker through a pathway in the MIP matrix, as seen in Fig. 1.4, resulting on an amperometric signal measurable in the electrochemical transducer [7, 22]. This approach was used in this work.

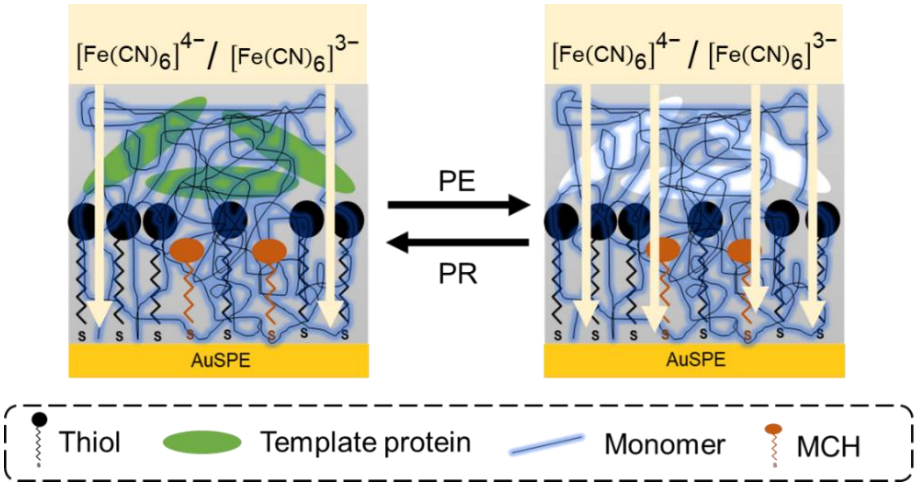

Figure 1.4 – Permeability of the redox marker through the MIP matrix, when protein extraction (PE) and protein rebinding (PR) occurs. Adapted from reference [7].

Electrochemical devices present major advantages, such as being easy to use, with a cost-effectiveness prodution and rapid and sensitive responses [2]. The possibility of miniturization of electrochemical bionsensors into small portable screen printed electrodes presents benefits in the application of this biosensors in PoC, with a lower cost of production and in most cases even disposable, a huge advantage for aplication in clinical diagnosis context [2].

1.2.2.1. Screen-printed Electrodes

Screen-printed electrodes (SPEs) are disposable devices obtained by printing different types of inks on a substrate, normally of ceramic or plastic nature. SPEs can be used with various types of electrochemical transducers, with main focus on the use of amperometric techniques for bioanalytical applications [23, 24].

Typically, a screen-printed electrode consists of a substrate with dimensions of approximately 3×1×0.05 cm, in which three or more electrodes are printed through screen-printing with a viscous ink, namely a working electrode, a pseudoreference electrode and a counter electrode (see Fig. 1.5) [23, 24]. The conductive path is normally covered with an insulator layer.

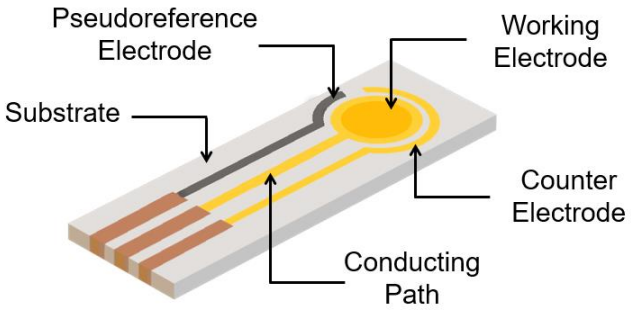

Figure 1.5 - Schematic representation of a gold screen-printed electrode (AuSPE).

The production of SPEs through screen-imprinting methodology is based on the deposition of viscous inks, ranging from 3 to 10 Pa·s, composed of metals or graphite. Depending on the desired type of electrode, a carbon, silver, or gold paste, also containing as binders, polymers, solvents, and other additives, can be used as a base for the electrode. They are deposited on a plastic or ceramic substrate equipped with a screen mesh, that determines the size and geometry of the electrodes. After the printing, the SPE is dried and cured. This production technique offers excellent reproducibility and design flexibility, allied to a low-cost of production due to mass production [23, 24].

The major point of interest of these small devices is the possibility of performing surface modifications of the working electrode, similarly to the conventional sized electrochemical cells, in order to provide selectivity to the system [24]. Specifically, in the fabrication of biosensors using SPEs, various materials have been used for the modifications of the working electrode, being enzymes and antibodies the main molecules immobilized through different processes [23, 24].

These devices associate well founded analytical methods with portability, allowing an effective application of this devices in PoC testing. Along with that main advantage, others can be pointed out, namely its simplicity and quick analysis, its reliability and repeatability, reproducibility of results, requiring low sample volumes (few microliters only) [23, 24].

1.3. State of the Art

Cancer is one of the world's leading cause of death, and its incidence is growing worldwide. Data consulted for the European continent for the year 2018 counted 3.91 million of new cases and 1.93 million deaths by cancer, meaning that 25% of the world population affected by this disease are Europeans [25, 26]. One of the best ways

to fight this silent disease is to work on early diagnoses, in order to provide best probabilities of cure and better life quality to the patients [25, 26].

Nowadays, biomarkers play a key role in the diagnose and follow-up management of cancer patients. The screening of the concentration profile of cancer biomarkers can be made through the analysis on different body fluids, such as blood, serum and urine, even before the appearance of any symptoms [2, 27].

Currently, immunoassays, like enzyme-linked immunosorbent assay (ELISA), are the most commonly used methods to detect cancer biomarkers in hospitals laboratories, allowing the detection of biomarkers with high sensitivity and selectivity [2, 27]. Nevertheless, these methodologies have the disadvantages of being expensive and based on laborious and time-consuming procedures [2, 4, 27]. In addition, biological antibodies are fragile (possible degradation and/or loss of antibody activity under acid/basic medium) and have a limited shelf life for quality assurance [2, 4, 27]. Therefore, there is currently a need to develop new simple, robust, fast, sensitive, and cost-effective methods for detection of cancer biomarkers in point-of-care (PoC) [4, 5].

Molecularly imprinted polymers (MIPs) allow the creation of synthetic biorecognition elements (plastic antibodies) capable of selectively bind to target complementary biomolecules, in a system analogue to the lock-and-key model developed by Emil Fisher [28]. Thus, MIPs present high specificity and selectivity to target molecules and can be obtained through simple and low-cost preparation methods. Besides, the rigid nature of the polymer matrix is physico-chemically stable, offering longer shelf-time than biological antibodies [6, 29].

Electrochemical biosensors are currently opening new horizons on the clinical and diagnosis field, due to their high sensitivity, ability to resist to different chemical environments, as well as being robust, easy to use, rapid and rather inexpensive comparing to other detection methodologies [2, 4, 5]. These biosensors also presents the unique benefit of being portable, allowing its use in PoC [2, 4, 5].

In the last decade, the use of MIPs for electrochemical biosensing has gain popularity due to its advantages and a major application of this technology is the development of new detection electrochemical devices for the detection of various cancer biomarkers in PoC [10-13].

In 2014, Rebelo *et al.* [21] described the use of MIP approach for the electroanalytical detection of prostate specific antigen (PSA). The binding sites were built through radical polymerization of vinylbenzene, in the presence of the template biomolecule, on a graphene electrode followed by enzymatic removal of the protein using a trypsin solution. This biosensor presented a linear response between 2.6 and

59.4 ng·mL^{-1} and a limit of detection (LOD) of 2 ng·mL^{-1} was obtained using potentiometric methods, below the reported cut-off value of 10 ng·mL^{-1} for PSA [21]. The biosensor was successfully applied for the detection of PSA biomarker in artificial serum. Furthermore, in 2018, Gomes *et al.* [11] reported the preparation of a MIP-based electrochemical biosensor for detection of carbohydrate antigen 15-3 (CA 15-3), by electropolymerizing O-phenylenediamine on a AuSPE using CV technique. After enzymatic extraction of the template molecule using a trypsin solution, rebinding studies for detection of CA 15-3 were performed. The biosensor had a linear concentration response range between 0.25 and 10.00 U·mL^{-1} and a LOD of 0.05 U·mL^{-1} was estimated using SWV, below the cut-off value of CA 15-3 (30 U·mL^{-1}). Successful results were obtained for detection of CA 15-3 on serum samples [11]. In another study, in 2018, Ribeiro *et al.* [13] reported the electroanalytical detection of the CA 15-3 biomarker by using MIP approach. The MIP surface was built by electropolymerization of poly(toludine blue) at the AuSPE surface also using cyclic voltammetry technique. The MIP was built over a toluidine blue-functionalized self-assembled monolayer (SAM) in order to increase the film stability at the electrode surface. The extraction of the template protein was achieved by incubating the prepared electrode surface with a sodium hydroxide solution, while performing CV cycles for effective washing. The rebinding experiences showed that the biosensor presented a linear response to CA 15-3 from concentrations between 0.1 to 100 U·mL^{-1}. A LOD below 0.1 U·mL^{-1} was achieved using differential pulse voltammetry (DPV) technique [13], allowing the application of the biosensor in clinical diagnosis context (CA 15-3 cut-off value: 30 U·mL^{-1}). The biosensor was successfully applied for the detection of CA 15-3 biomarker in artificial serum. Finally, Pacheco *et al.* [12], also in 2018, published a work reporting the development of new MIP-based electrochemical device for detection of breast cancer biomarker human epidermal growth factor receptor 2 (HER2-ECD). The MIP surface was prepared by CV electropolymerization of phenol in the presence of the target protein, on a AuSPE. Posterior extraction of the HER2-CD was achieved by incubating the prepared biosensor surface with a solution composed of sodium dodecyl sulphate (SDS) 0.5% and acetic acid 0.5%. This device showed a linear response range between 10 and 70 ng·mL^{-1}. From the calibration plot, a LOD of 1.6 ng·mL^{-1} was obtained using differential pulse voltammetry (DPV) technique, bellow the cut-off value for HER2-CD (15 ng·mL^{-1}) [12]. The biosensor was successfully applied for detection of the cancer biomarker in serum samples.

The main objective of the present work was the development of a new MIP-based electrochemical device for detection of cancer biomarkers with high sensitivity and selectivity, using AuSPEs as transducers for PoC analysis.

1.4. Techniques of Surface Characterization

1.4.1. Electrochemical techniques

Electrochemistry and electroanalytical chemistry fields are constantly evolving to better understand reactions occurring at the electrode surface using various methods, namely by the measurement of changes in electric current (amperometric methods), potential (potentiometric methods) or even in the conductance (conductometric methods) [30, 31].

In this work two amperometric techniques, cyclic voltammetry (CV) and square wave voltammetry (SWV), were used for surface characterization during the step-by-step preparation of sensor surfaces. In addition, SWV was also used as quantification technique to evaluate the biosensor performance. The electrochemical measurements were performed in the presence of a ferrocyanide/ferricyanide redox probe solution to monitor the peak current decrease due to the surface block to redox probe permeation to the film deposited at the electrode surface.

1.4.1.1. Cyclic Voltammetry

CV is a voltammetric method where the potential applied on an electrode is linearly changed in function of time, with a defined scan rate, from an initial value (E_{start}) until a switching potential (E_λ) (see Fig. 1.6a), while recording the current flow in the electrochemical cell (see Fig. 1.6b) [31-33]. Furthermore, the typical CV voltammogram obtained for the reversible system ferrocyanide/ferricyanide redox couple is shown in Fig. 1.6c. As can be seen in the figure, to identify the anodic and cathodic current peaks, that corresponds to peak height measured, tangents to the baseline of each sweep were established from this purpose.

Fig. 1.6a represents the plot of the cyclic linear potential sweep applied to the system. This plot is characterized by its symmetry, since both forward and reverse sweeps are symmetrical by the switch or inversion point (E_λ) [34]. The system current response to the potential applied can be observed in the Fig. 1.6b. The potential switching point, E_λ, coincides with the inversion point of the current-time plot where the anodic current is converted in cathodic current. Since both, potential and current plots,

correlate equally with time, a representation of current versus potential plot can be represented (see Fig. 1.6c), commonly known as CV voltammogram [34].

The voltammogram shown in Fig. 1.6c represents a typical profile of a reversible system ranging from smaller to higher potentials. According to the IUPAC convention, the positive current refers to the anodic processes (oxidation) that occur in the electrochemical cell. Thus, the anodic peak ($I_{p,a}$) observed in Fig. 1.6c corresponds to the oxidation of ferrocyanide $\left[Fe(CN)_6^{-4}\right]$ to ferricyanide $\left[Fe(CN)_6^{-3}\right]$ [30, 34]. After the inversion point, the potential scan is negative, and reduction reaction of ferricyanide back to ferrocyanide at the surface of the electrode occurs giving origin to the cathodic current peak ($I_{p,c}$) represented in the figure [30, 34].

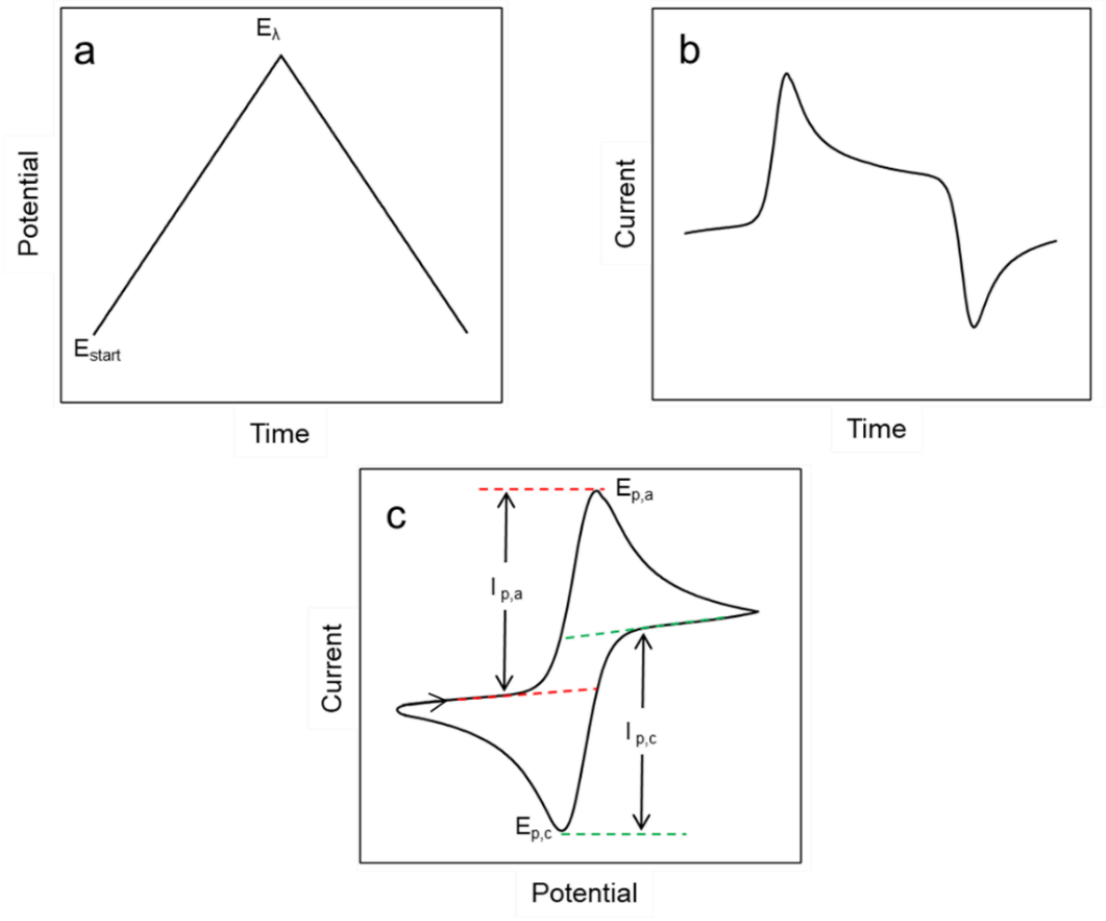

Figure 1.6 - Representation of the typical plots (a) potential applied vs. time, (b) current vs. time (c) current vs. potential (CV voltammogram) obtained for the ferrocyanide/ferricyanide redox couple probe at the gold screen printed electrode, data collected during experimental procedures.

From an experimental point of view, it is common practice that the formal potential ($E^{0'}$) can be calculated using the anodic and cathodic peak potentials obtained in CV voltammogram recorded of the redox couple and using equation 1.1 [32, 33, 35].

$$E^{0'} = \frac{E_{pc} + E_{pa}}{2} \qquad \text{Equation 1.1}$$

This approximation is most accurate when the electron transfer process is reversible, and the diffusion coefficients are the same for the oxidized and reduced species [32]. For reversible reactions, the separation in the peak potentials is close to 59/n mV (at 25 ^{o}C) [30], where *n* represents the number of electrons involved in the redox reaction. Thus, this relationship can be used to evaluate *n* [32].

According to the above theory, the separation between anodic and cathodic peaks corresponds to 59 mV (at 25 ^{o}C) for the reversible ferrocyanide/ferricyanide redox couple at a perfect gold surface, since the rate of the reaction is governed by diffusion, and only one electron (*n*=1) is involved in the reaction. Under our experimental conditions, a separation of peaks potentials of ~76 mV was obtained, at a 50 $mV \cdot s^{-1}$, which is close agreement with values reported in literature [36]. This experimental value is slightly higher than the predicted for a Nernstian one-electron reaction (59 mV) suggesting some influence of the type of electrode used (SPE) and ink composition (lower percentage of elemental gold when compared to conventional electrodes) on the electron transfer kinetics [37].

Moreover, the formal potential ($E^{0'}$) of the ferrocyanide/ferricyanide redox couple was reported to be 0.56 V (at 25 ^{o}C, using a 0.1 $mol \cdot L^{-1}$ HCl solution as electrolyte) [30] while a formal potential ($E^{0'}$) of ~0.094 V was estimated for the ferrocyanide/ferricyanide redox at the bare AuSPE surface (using a 0.1 $mol \cdot L^{-1}$ Na_2SO_4 solution as electrolyte).

Furthermore, the reversibility of the system can be studied by analysing the ratio between the theoretical and experimental values of the cathodic and anodic peak currents [30].

$$\frac{|I_{p,a}|}{|I_{p,c}|} = 1 \qquad \text{Equation 1.2}$$

For our experimental redox system, ratio between the peak currents is 1.1, confirming that the redox reaction is fully reversible.

The rate defined for the variation of the applied potential, known as scan rate, is an important experimental parameter since a fast scan can result in a decrease in the size of the diffusion layer, resulting in higher values of current measured [32, 33].

For a redox system where a reversible process regulated by diffusion occurs, at 25 ^{o}C, the peak current intensity, I_p can be calculated using the Randles-Sevčik equation:

$$I_p=2.686\times10^5 n^{3/2} A c_0 D^{1/2} \nu^{1/2} \quad \text{Equation 1.3}$$

where *n* is the number of electrons involved in the reaction, *A* is the electrode area (in cm^2), *D* is the diffusion coefficient (in $cm^2 \cdot s^{-1}$), c_0 is the concentration of species (in $mol \cdot cm^{-3}$) and ν is the scan rate (in $V \cdot s^{-1}$) [30, 32, 33, 38]. Thus, considering the above equation there must exist a linear correlation between the peak current intensity and the square root of the scan rate. Finally, it is also important to notice that the peak current intensity increases linearly with the concentration of species in solution [30, 32].

1.4.1.2. Square Wave Voltammetry

In SWV, a potential pulse is applied to an electrode in function of time (see Fig. 1.7a), that varies in an amplitude ΔE_p, superimposed by a staircase waveform with a step potential ΔE_s [30, 38-40]. The measured response signal, current $I_{peak(SWV)}$, is calculated as the difference between the peak current measured for a forward and reverse pulse applied to the system (see Fig 1.7b). The forward current, I_F, corresponds to the measurements made at the end of the first pulse in the direction of the scan, while the reverse current, I_R, is measured at the end of the second pulse in the opposite direction of the scan [38-40]. In Fig. 1.7b the anodic current peak observed corresponds to the oxidation of ferrocyanide to ferricyanide during the forward scan [30].

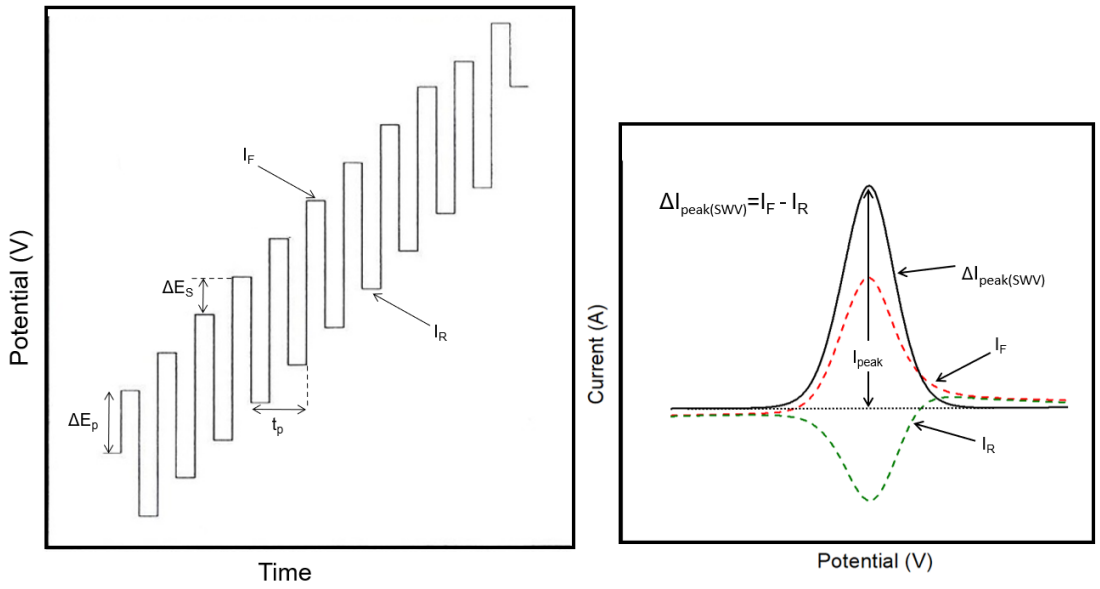

Figure 1.7 - Representation of the typical plots (a) potential applied vs. time (adapted with consent from [41]), (b) current vs. potential (SWV voltammogram) obtained for the ferrocyanide/ferricyanide redox couple probe at the gold screen printed electrode (AuSPE) surface, data collected during experimental procedures..

For plane electrodes, the peak current intensity can be calculated using Aoki *et al.* theory:

$$\Delta I_p = 0.9653 n F A c \left(\frac{D}{\tau}\right)^{1/2} \tanh\left(\frac{\zeta}{2}\right) \qquad \text{Equation 1.4}$$

where n is the number of electrons involved in the reaction, F is the Faraday constant (F= 96485 C·mol^{-1}), A is the electrode area (in cm^2), c is the species bulk concentration (in mol·m^{-3}), D is the diffusion coefficient (in cm^2·s^{-1}), τ is the square wave period (in s), and ζ is the dimensionless electrode potential [40]. Thus, according to equation 2.4, the experimental parameters that can influence the SWV analysis are the amplitude (ΔE_p), the step potential (ΔE_s), the square wave frequency (f) and the equilibration time [41, 42]. From these parameters, both, pulse amplitude and frequency, have a huge contribution on the sensitivity and peak resolution obtained using this technique [30, 42].

SWV has been widely used in electroanalytical studies for detection of various biochemical molecules, such as aminoacids, cancer biomarkers and proteins in carbon and gold modified electrodes [43-46]. Other electrochemical techniques have been used for the same purpose, such as the differential pulse voltammetry (DPV) and CV, however, SWV has shown better performance since it allows the collection of well-defined current peaks with higher sensibility and faster time of analysis (of few seconds only) [30].

2. Experimental Details

2.1. Experimental Apparatus

2.1.1. Reagents and Solutions

2.1.2. Electrochemical Apparatus

2.1.3. Electrochemical Measurements

2.1.4. Biosensor Preparation

2.1.5. Analytical Performance of the Biosensor

2. Experimental Details

2.1. Experimental Apparatus

In this chapter, the biosensor preparation for detection of cancer biomarkers and electrochemical surface characterization is described, as well as the subsequent study of the biosensor analytical performance.

2.1.1. Reagents and solutions

All the thiols, proteins and aminophenol used in this work are listed on table 2.1, as well as the provenience and the quality. This list presents also all the reagents used for preparation of standard stock solutions.

All the aqueous solutions used were prepared using water purified with a Milli-Q purification system (resistivity ≥ 18MΩ cm). A 0.1 mol·L^{-1} phosphate buffer solution (PBS) (at pH 7.4) and an acetate buffer solution (ABS) 0.1 mol·L^{-1} (at pH 4.0) were freshly prepared prior to the experiments. A 500 µmol·L^{-1} BSA solution in 0.1 mol·L^{-1} PBS (at pH 7.4) was used as a template protein standard solution.

Table 2.1 - List of reagents used.

Name	Acronym / Molecular formula	Quality (%)	Company
3-aminophenol	APh	98	Sigma-Aldrich
6-Sulfhydryl-hexane-1-ol	MCH	97	Aldrich Chem
8-Amino-octane-1-thiol	AOT	≥90	Dojindo Laboratories
Hexane-1-thiol	HT	96	Alfa Aesar
Sodium dodecyl sulphate	SDS	≥99	Merck
Bovine serum albumin	BSA	≥96	Sigma-Aldrich
Sodium dihydrogen phosphate dihydrate	$NaH_2PO_4 \cdot 2H_2O$	p.a.	Sigma-Aldrich
Anhydrous disodium hydrogen phosphate	Na_2HPO_4	p.a.	Fluka
Sodium acetate	$NaCH_3COO$	p.a.	Sigma-Aldrich
Sodium hydroxide	NaOH	98	Merck

Acetic acid	CH_3COOH	≥99	Sigma-Aldrich
Potassium ferricyanide	$K_3[Fe(CN)_6]$	≥99	Fluka
Potassium ferrocyanide	$K_4[Fe(CN)_6].3H_2O$	≥99.5	Fluka
Sodium sulphate	Na_2SO_4	p.a.	Fluka
Dimethyl sulfoxide (dried)	DMSO	≥99.9	Sigma-Aldrich
Hexaammineruthenium(III) chloride	HAR	98	Aldrich
1,1'-ferrocenedimethanol	FDM	98%	Aldrich

2.1.2. Electrochemical Apparatus

Electrochemical data was obtained using a computer-controlled potentiostat Autolab PGSTAT30 (Eco Chemie B.V., Utrecht, Netherlands, Fig. 2.3a) monitored by the NOVA 2.1.3 software package.

Gold screen-printed electrodes (AuSPEs, Fig. 2.3b) were purchased from Metrohm (DropSens DRP-220AT). They include a gold disk-shaped working electrode (geometrical area of 12.6 mm^2), a pseudo-reference electrode based on a silver ink and a gold counter electrode, all screen-printed on a ceramic substrate (3.3×1.0 cm) and subjected to high-temperature curing. All potential values are referred to the screen-printed silver pseudo-reference electrode. The electric contacts are also made of a silver ink.

The AuSPEs were connected to a switch box from DropSens (DRP-DSC, Fig. 2.1c), allowing to connect their interface with the potentiostat. All experiments were carried out at room temperature.

The collected data was processed using the software OriginPro 9.0.0.

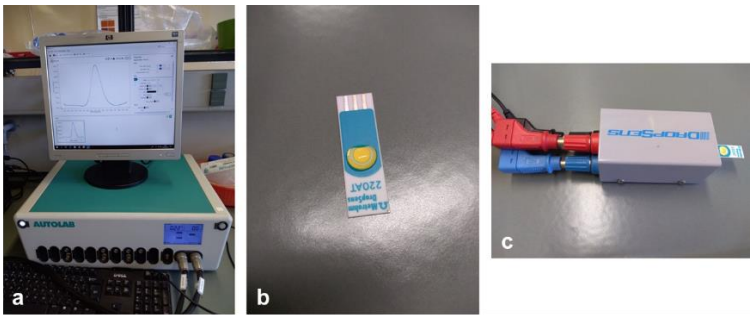

Figure 2.1 - (a) Computer-controlled potentiostat Autolab PGSTAT30. (b) DropSens' gold screen-printed electrodes (AuSPE). (c) DropSens' switch box.

2.1.3. Electrochemical Measurements

The redox probe used for the surface characterization and quantification studies was a 5 mmol·L^{-1} ferrocyanide/ferricyanide solution. This solution was prepared with equimolar concentrations of potassium ferricyanide and potassium ferrocyanide, dissolved in a 0.1 mol·L^{-1} sodium sulphate electrolyte solution.

Both CV and SWV were recorded in the potential range of −0.30 V to 0.50 V. CV was performed at a scan rate of 50 mV·s^{-1} and SWV operated with a step potential of 2 mV, pulse amplitude of 50 mV and frequency of 25 Hz.

2.1.4. Biosensor Preparation

The AuSPEs were firstly washed with pure water, followed by ethanol and acetone, the procedure was repeated three times. Then, the chips were dried under a nitrogen flow.

The electrochemical cleaning of the electrode surface before modification was performed by using CV technique in 0.1 mol·L^{-1} sulfuric acid (H_2SO_4) solution. A 60 µL drop of this solution was placed on top of the chip covering all the three electrodes. CV cycles were performed between 0 to 1.15 V, at a scan rate of 0.1 V·s^{-1}, until the voltammogram was stable, which took approximately ten cycles. After the electrochemical cleaning, the AuSPEs were washed with pure water and dried under nitrogen flow. This procedure was repeated after each surface modification step and electrochemical measurement .

As stated before, bovine serum albumin (BSA) was used as template molecule in our preliminary studies for optimization of the biosensor preparation procedures. Furthermore, SAM approach was used in this work for template protein immobilization and to control non-specific adsorption at the electrode surface. SAMs of hexane-1-thiol (HT) and 8-amino-octane-1-thiol (AOT) were deposited at the working electrode surface for effective template protein immobilization at electrode surface prior to molecular imprinting, while 6-sulfhydryl-hexane-1-ol (MCH) was used for reduction of non-specific adsorption after target protein electropolymerization at the electrode surface.

A non-imprinted polymer (NIP) was also prepared on the AuSPEs, with the purpose to provide a reference system not capable of recognizing the target protein through specific adsorption, since specific binding sites could not be created in the absence of target protein immobilized on the surface when monomer electropolymerization occurs. The MIP-based sensor surface was prepared according to the procedure schematically represented in Fig. 2.2, and includes the following steps:

A – Incubation overnight of the working electrode with a 15 µL drop of a 1 mmol·L^{-1} thiol solution.

B – Incubation for 2 hours of the working electrode covered with the pre-formed SAM with a 15 µL drop of a 500 µmol·L^{-1} BSA solution.

C/D – Electropolymerization of 3-aminophenol (APh), using CV technique, after covering the electrode surface with a 60 µL drop of a 500 µmol·L^{-1} Aph solution in PBS. The CV was performed by cycling potential from -0.2 V to 0.65 V, at a scan rate of 0.1 V·s^{-1}. The number of cycles performed was optimized in order to control the polymerized film thickness.

E – Incubation for 2 hours of AuSPE surface with a 60 µL drop of a 1 mmol·L^{-1} MCH solution.

F – Immersion overnight of the AuSPE in a 25 mmol·L^{-1} acidic SDS solution, prepared in ABS.

Before each modification step, the electrochemical surface characterization was performed using CV and SWV techniques and the ferrocyanide/ferricyanide redox couple as reporting system.

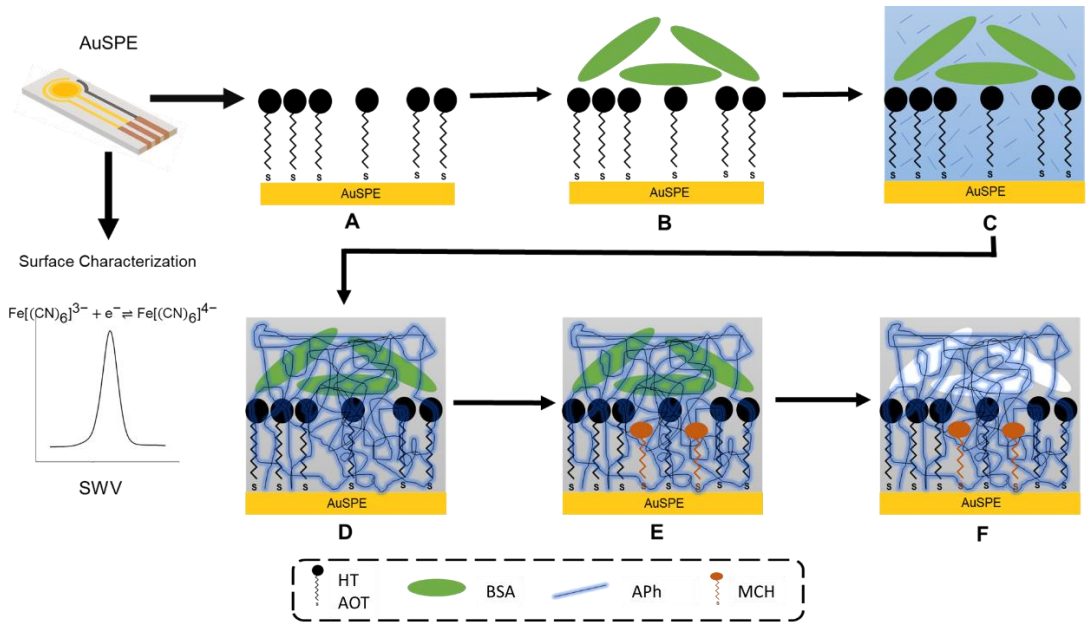

Figure 2.2 - Methodology used for the preparation of MIP sensor surfaces: **(A)** Thiol SAM formation overnight. **(B)** BSA deposition for 2 hours. **(C-D)** Creation of the specific binding sites by electropolymerization of the APh using CV technique. **(E)** MCH incubation for 2 hours. **(F)** BSA extraction from the polymeric matrix with SDS overnight. A non-imprinted polymer (NIP) acting as control was also prepared using the same techniques as the MIP, except for step (B) in which the incubation was made with PBS instead of BSA.

2.1.5. Analytical performance of the sensor

Prior to the detection studies, the sensor surface was incubated with PBS (without BSA) for 2 minutes and washed with pure water, followed by electrochemical measurements in the presence of 5 mmol·L^{-1} ferrocyanide/ferricyanide redox couple, in order to collect the system baseline (MIP and NIP). This procedure was repeated until stable baselines were obtained (variation of the peak intensity is almost null) and avoid signal variation due to buffer solution components.

After evaluation of the sensor stability and collect the baseline, the electrode surface was incubated for 30 minutes with the standard BSA solution with increasing concentration of target protein (from 1 nmol·L^{-1} to 100 µmol·L^{-1}), followed by surface washing with pure water. Then, SWV measurements in the presence of the ferrocyanide/ferricyanide redox couple were performed over the sensor surfaces (MIP and NIP electrodes) after the incubation step. The peak current intensity obtained by SWV (using NOVA software data treatment tools) was represented as a function of the logarithm of the BSA concentration. From the obtained calibration curve, the limit of detection (LOD) of the sensor was estimated.

3. Results and Discussion

3.1. Redox Probe Selection

3.2. Biosensor Preparation

3.2.1. Thiol Selection for Immobilization of the Template

3.2.2. MIP Preparation by Electropolymerization

3.2.2.1. Electropolymerization of 3-aminophenol

3.2.2.2. Protein Extraction

3.2.2.3. Thickness of 3-aminophenol Film

3.3. Quantification Studies

3. Results

This work was developed in two distinct phases: (i) firstly, the experimental conditions for the preparation of the biosensor were optimized, followed by (ii) evaluation of the biosensor performance.

Since the surface modification procedures and protein detection were monitored by indirect electrochemical measurements in the presence of a suitable redox probe, it is important to evaluate the stability of redox probe signals at a bare AuSPE surface, in order to obtain accurate and reproducible results.

3.1. Redox Probe Selection

One of the simplest and cost-effective approaches for detection of biomolecules using electrochemical biosensing devices is to monitor the permeability of a low molecular weight redox probe through the MIP film. Therefore, it's fundamental for the successful performance of electrochemical biosensors that the chosen biocompatible redox probe can provide a stable and reproducible response.

Although the ferrocyanide/ferricyanide redox couple has been extensively used as reporting system in electrochemical biosensors for detection of cancer biomarkers [1-3], some issues related to this reporting system have been described in literature [4], namely: (i) poisoning of the gold electrode surface due to the irreversible adsorption of redox species and/or secondary products; (ii) decomposition of the redox probe in the presence of chloride ions and; (iii) thiol instability in the presence of the ferrocyanide/ferricyanide redox couple.

In this work, the signal stability of three diffusional redox systems, ferrocyanide/ferricyanide redox couple, hexaammineruthenium (HAR) and ferrocenedimethanol (FDM), was studied at the bare AuSPE surface using electrochemical techniques and electrochemistry combined-surface plasmon resonance (eSPR).

CV and SWV were selected for the studies since they are two routinely used techniques in the electroanalysis studies, while eSPR technique can evaluate the possible formation of redox probe complexes (and/or secondary products) at the gold electrode surface.

The redox probe signal stability was evaluated under two electrochemical conditions, by performing (i) 10 repetitive SWV measurements over the same electrode

surface or (ii) 10 measurements consisting of three CV cycles followed by SWV measurement (CV+SWV).

The results of this study were recently published earlier this year in a research paper by Ribeiro *et al.* [47] (see Annex 1).

Briefly, based on the results obtained for each reporting systems we were able to conclude that acceptable signal variability over repetitive measurements was obtained at the bare AuSPE surface, with FDM being the exception, (see Fig. 3 of the publication), meaning that no significant irreversible adsorption of redox species occurs at the electrode surface under the conditions tested. The redox probe $I_{peak(SWV)}$ signal variability relatively to the initial value was inferior to 13% and the relative standard deviation (RSD) values were inferior to 5% for all the redox probes tested, with the exception of the FDM redox probe, that presents a RSD of 8.9% when CV+SWV was performed (meaning that CV technique should be avoid for this probe at the AuSPE surface). Moreover, although a stable response was observed for HAR at the bare AuSPE surface, an undesired drift of the potential over repeated measurements occurred (see Fig. S3 and Fig. S4 in Supporting Information of the publication, Annex 1). Thus, considering the above-mentioned results, the ferrocyanide/ferricyanide couple was chosen as redox reporting system in this work.

In the published work, a simple methodology based on SWV technique was used to obtain information about the diffusional behaviour of the redox probes studied before and after AuSPE surface modification with an AOT SAM and an electropolymerized film of poly(3-aminophenol) (see Fig. 4A of the publication). The continuous decrease of the variation of the amplitude-normalized peak current in SWV ($I_{peak(SWV)}/\Delta E_p$) *vs.* the pulse amplitude (ΔE_p) for the ferrocyanide/ferricyanide redox couple indicated that reversible diffusion behaviour is maintained after surface modification with AOT SAM and poly(3-aminophenol), two modification steps used in this work to build the MIP film.

Some experimental details related to the use of redox probes on AuSPEs were also considered in this work, namely: (i) use of a chloride-free electrolyte (to avoid potential drift and/or the formation of secondary products at the electrode surface); (ii) use of solutions at low concentration levels of redox couple (between 1 and 5 $mmol \cdot L^{-1}$), while keeping the solution protected from daylight and (iii) minimization of the number of electrochemical measurements, incubation time, measurement time and potential limits.

Thus, CV and SWV techniques, in the presence of ferrocyanide/ferricyanide redox couple, were selected in this work to monitor the surface modification procedures. To perform the biosensing studies, SWV was chosen since it performs the

measurements rapidly (low incubation times) with high sensitivity. Besides, SWV allows to obtain a better peak resolution comparing to CV (similar to a chromatographic peak) which is an advantage when performing quantification studies, allowing simple and easy collection of analytical data.

3.2. Biosensor Preparation

Various parameters were considered during the optimization of the biosensor preparation, namely the selection of the thiol used for the template protein immobilization, the experimental parameters concerning the electropolymerization of 3-aminophenol monomer, and the protein extraction.

3.2.1. Thiol selection for immobilization of the template

As stated before, SAM approach was used for immobilization of the template protein at the AuSPE surface since the strong chemisorption of the sulfur atoms of the thiol to the gold electrode surface (covalent bond) [5] can provide a stable organic layer to support the protein (avoiding its denaturation).

In this work, two thiols, 8-amino-octane-1-thiol (AOT) and hexane-1-thiol (HT), where chosen for the formation of a SAM on the AuSPE substrates AOT presents an hydrophilic nature due to the terminal amino group while HT presents hydrophobic terminal groups ($-CH_3$). A 1.0 $mmol \cdot L^{-1}$ aqueous solution of AOT and 1.0 $mmol \cdot L^{-1}$ solution of HT, dissolved in DMSO, were used for adsorption of the thiol on the working electrode (10 µL drop) overnight. The chips were left on a glass container to prevent solution evaporation.

Then, the SAM modified surface was incubated with a 500 $\mu mol \cdot L^{-1}$ BSA solution (in 0.1 $mol \cdot L^{-1}$ PBS at pH 7.4) for 2 hours for immobilization of the template protein.

CV and SWV measurements were performed to evaluate the preparation of the SAM surfaces and the template immobilization. The typical SWV voltammograms recorded are shown in Fig. 3.1. As can be seen in the figure, after incubating the clean AuSPEs working area with the thiol solutions, a decrease of the peak current intensity was observed due to the increased difficulty of the redox couple to reach the electrode surface after SAM deposition, therefore, confirming the successful preparation of both, AOT and HT, SAM surfaces. Furthermore, an additional decrease of the peak current intensity was observed after incubation of the surface with the protein solution, revealing

that BSA can be adsorbed in SAMs having different terminal groups through hydrophilic or hydrophobic interactions.

The typical CVs obtained under the same experimental conditions were also collected, however, the differences in peak current intensity after the SAM deposition (and immobilization of BSA) were not so perceptible as in SWV and the data was not presented for discussion (CVs obtained can be consulted in Annex 2).

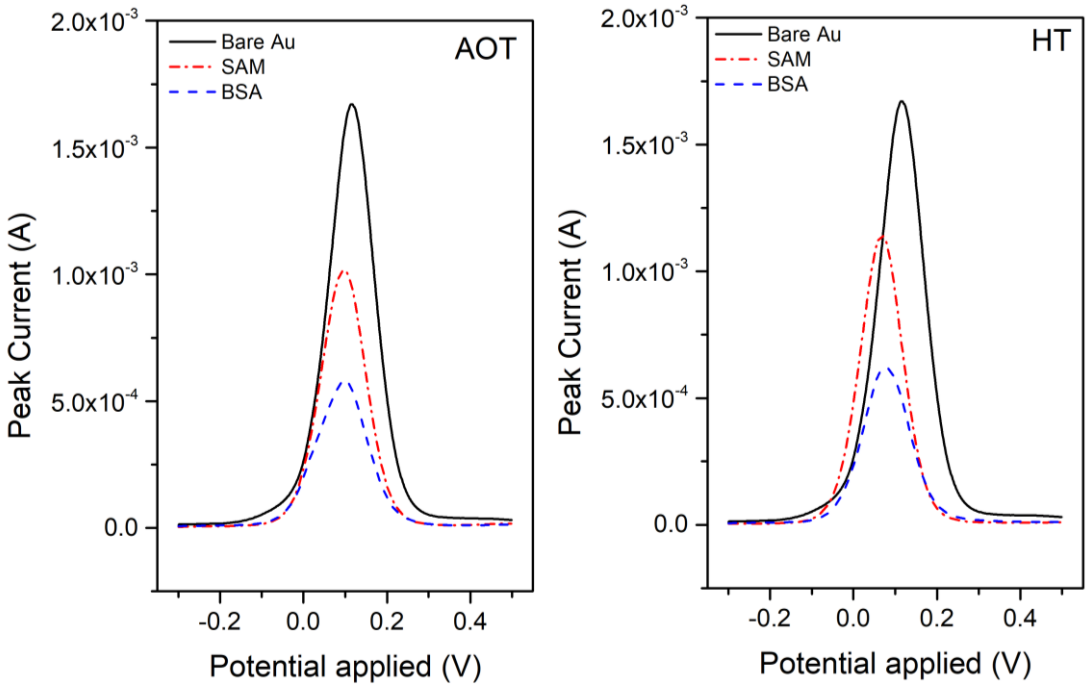

Figure 3.1 – Typical SWVs obtained at the AuSPE surface, in the presence of a 5 mmol·L^{-1} redox probe solution, (black) before and (red) after surface modification with SAMs of (left) AOT and (right) HT, following by (blue) BSA immobilization.

Considering the repetitive modification experiements made on the AuSPEs, the mean values obtained for the redox probe peak current intensity are presented in Fig. 3.2. Data obtained allowed to conclude that both thiols monolayers, AOT and HT, were successfully formed at the chip surface. The similar SAM blockage to the redox probe can be explained by the similar length of the thiols carbon chains (C8 and C6, for AOT and HT, respectively). Higher chain length thiols were not selected to build the SAM monolayer in this work in order to prevent excessive redox probe blocking that could compromise the electrochemical response.

Moreover, HT SAM allowed the adsorption of a slightly higher amount of BSA than AOT. However, the difference is not significant since it is less than 10%.

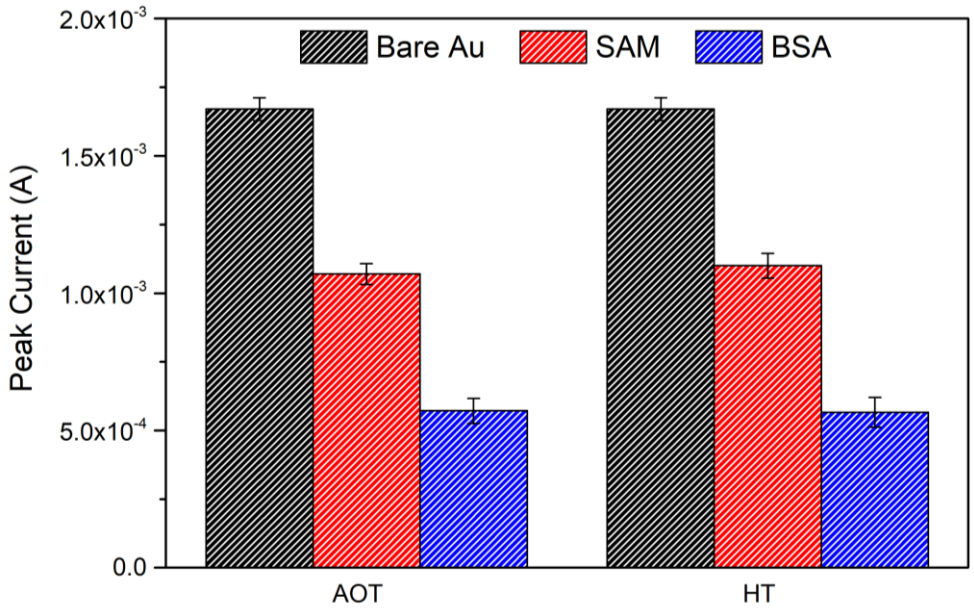

Figure 3.2 - Mean values of SWV peak current intensity obtained at the (black) bare AuSPE, (red) SAM/AuSPE, and (blue) BSA/SAM/AuSPE. The error bars were obtained from 3 independent repetitions of the experiment.

SPR experiments were performed in collaboration with the investigation group in order to obtain more information about BSA adsorption on SAM surfaces (see annex 3). The SPR results supported the electrochemical data obtained, showing that AOT and HT monolayers can immobilize similar amounts of protein (although a slight advantage was observed for HT). Furthermore, the SPR measurements allow to conclude that the protein immobilization at the SAM surface is reversible, since extraction with acidic SDS solution resulted on a decrease of the measured angle to the initial baseline values, meaning that the protein immobilized on the SAM was extracted. On other hand, the SPR results also allowed to conclude that for BSA concentrations above 250 $\mu mol \cdot L^{-1}$, the SPR angle didn't show significant variations. The optimal BSA solution concentration chosen was of 500 $\mu mol \cdot L^{-1}$ to assure maximal immobilization of protein at the SAM surface.

Since both, AOT and HT, SAMs allowed the immobilization of similar amounts of BSA, the toxicity of each compound and its solubility in water was also considered. HT was only soluble in DMSO and is severely hazardous (e.g., harmful when swallowed, toxic if inhaled) [48]. Thus, AOT thiol was chosen for BSA immobilization without compromising the amount of protein bound to the electrode surface.

3.2.2. MIP Preparation by Electropolymerization

After the immobilization of the template protein, the 3-aminophenol monomer was selected for the electropolymerization process, using CV technique, in other to create the specific binding sites.

3.2.2.1. Electropolymerization of 3-aminophenol

As stated before, the MIP film was prepared by using an electrochemical technique. Fig. 3.3a shows the typical CV profile for the electropolymerization of a 3-aminophenol (APh) monomer (C = 500 µmol·L^{-1}, 0.1 mol·L^{-1} PBS at pH 7.4) on a bare AuSPE surface. Three CV cycles were recorded using a potential window between -0.3 and 0.75 V at a scan rate of 100 mV·s^{-1}.

As can be seen in the figure, the (irreversible) oxidation of 3-aminophenol monomer occurs near the positive end of the potential window (at ~0.39 V) and corresponds to the loss of one electron from the nitrogen atom lone pair, allowing the formation of a non-conductive polymer film at the electrode surface [8-10]. The proposed mechanism for electropolymerization of poly(3-aminophenol) is schematically represented in Fig. 3.3b. The decrease of the peak current intensity between each cycle is justified by the increasing blocking effect to monomer diffusion caused by the growing polymer film at the electrode surface [10].

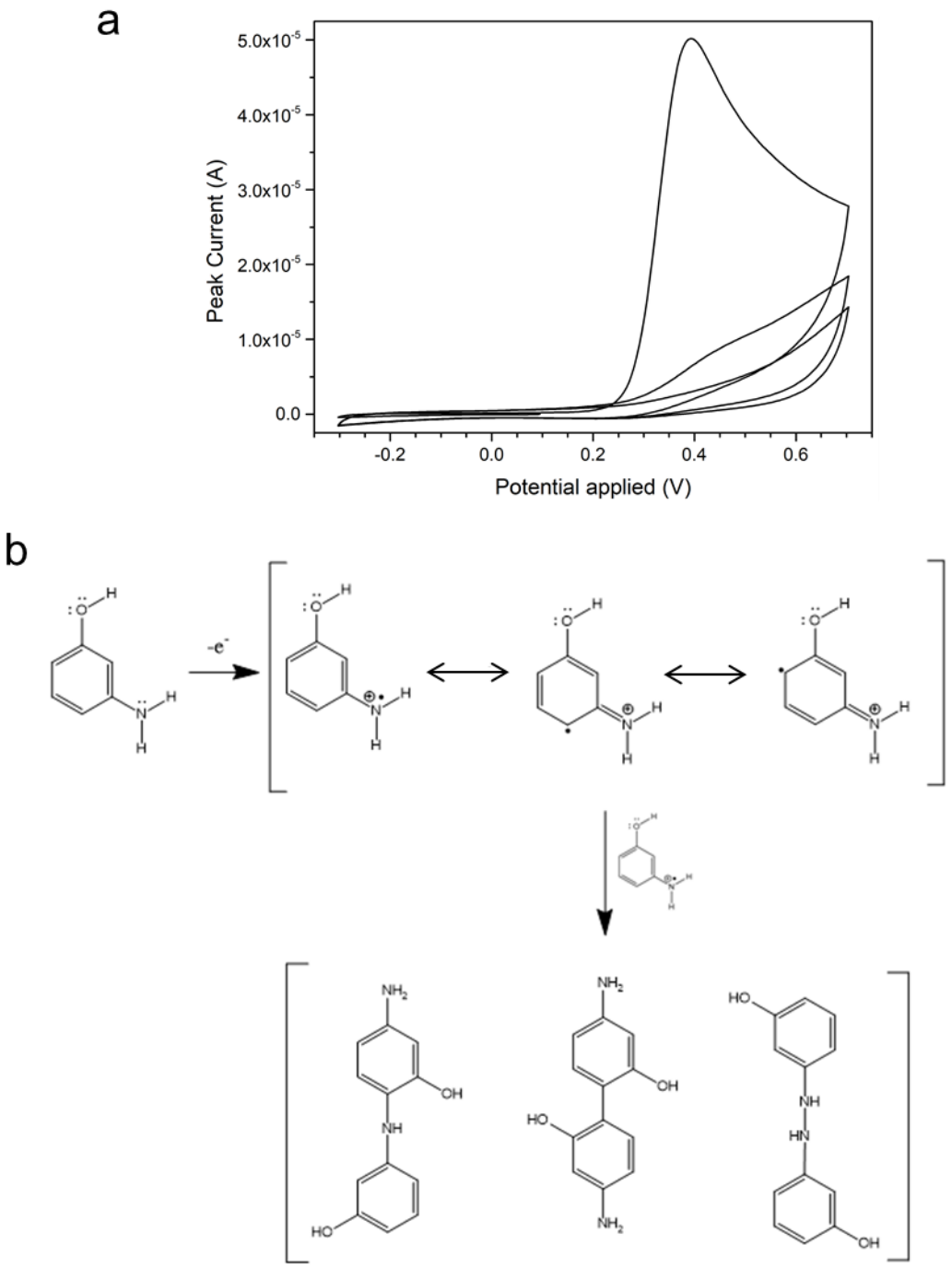

Figure 3.3 – (a) Typical CV voltammogram obtained for the electropolymerization of a 500 µmol·L^{-1} 3-aminophenol monomer solution (prepared in 0.1 mol·L^{-1} PBS at pH 7.4) on a bare AuSPE surface. Number of cycles: 3; scan rate: 100 mV·s^{-1}. (b) Proposed mechanism for the electropolymerization of 3-aminophenol. Adapted from [49].

3.2.2.2. Protein extraction

In this work, the extraction of the template protein was attempted by using a basic solution (0.1 mol·L^{-1} NaOH) or buffer solutions (at pH 7.4 and pH 4.0) containing SDS at a concentration of 25 mmol·L^{-1}.

Studies were performed firstly on the NIP surface to evaluate SAM and polymer stability in the presence of extraction solutions. From the preliminary experiments performed, it was possible to conclude that NaOH partially destroyed the NIP surface, either by attacking the polymer and/or the thiol monolayer. On the other hand, the two SDS solutions at different pH values tested revealed to maintain surface integrity (see annex 4).

The experiments performed on the MIP surface revealed that the acidic SDS solution induces a greater protein extraction from the polymer matrix than the neutral SDS solution. This phenomenon is probably related with the change in native protein conformation when pH changes to acidic values. BSA isoelectric point is between 4.5 and 5.0 [1], meaning it is negatively charged under physiological conditions. At pH 4.0, the protein becomes positively charged due to the protonation of amine groups, resulting in the change in protein conformation inside the binding sites due to electrostatic repulsion, thus, facilitating the protein extraction. Furthermore, it becomes easier for the negatively charged SDS micelles to be around the protein and contributes to protein unfolding [50].

Moreover, the 3-aminophenol monomer has a pK_a value of 4.37 [51], thus, being neutral under physiological conditions. However, during the extraction process, the medium pH changed to values bellow its pK_a and the amino functional groups at the polymeric film become protonated. This change in polymer charge, associated to the protonation of the amino groups of BSA, is expected to cause electrostatic repulsions between the protein and the polymeric matrix, making the extraction of the template protein easier.

In this work, the effective extraction of BSA was achieved by incubating the chips overnight with a 25 mmol·L^{-1} SDS prepared in 0.1 mol·L^{-1} ABS at pH 4.0.

3.2.2.3. Thickness of the MIP film

The thickness of the electropolymerized film should, in theory, match the template protein size to increase the performance of the prepared biosensor, since films too thin can lead poor imprinting (lack of selectivity) while films too thick can compromise protein extraction of the MIP matrix (lack of sensitivity) [15].

Various parameters, such as the number of cycles performed, or the potential scan rate chosen for the CV electropolymerization, can influence the thickness of the electropolymerized MIP film [15].

In this work, the optimization of the thickness of the electropolymerized 3-aminophenol film was controlled by the number of cycles (1, 2 and 4 cycles) performed during CV electropolymerization, while keeping the scan rate constant (at 100 $mV \cdot s^{-1}$).

The typical CV voltammograms for the electropolymerization of 3-aminophenol monomer obtained for both systems,MIP and NIP, are presented in Fig. 3.4. Two CV cycles were performed at the AOT SAM/AuSPE surface. The similar CV voltammograms for the electropolymerization using one and four CV cycles are represented in annex 5. As can be seen in the figure, a lower peak current intensity due to monomer oxidation was obtained at the MIP surface relatively to the NIP surface, which is due to the BSA immobilized at the SAM surface that caused an additional diffusional barrier to monomer oxidation at the electrode surface [1].

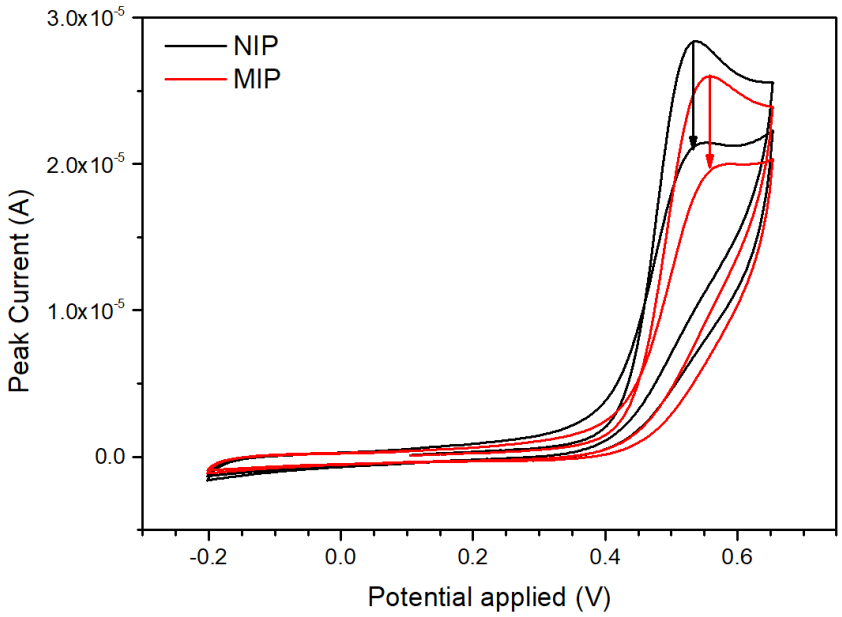

Figure 3.4 – Typical CV voltammograms obtained for of electropolymerization of 3-aminophenol monomer solution (C = 500 $\mu mol.L^{-1}$, in 0.1 $mol \cdot L^{-1}$ PBS at pH 7.4) at the (black) NIP and (red) MIP surfaces. Number of cycles: 2, scan rate: 100 $mV \cdot s^{-1}$.

Furthermore, the step-by-step preparation of the biosensor was monitored by electrochemical techniques. The recorded SWVs are shown in Fig. 3.5 for both, NIP (Fig. 3.5a) and MIP (Fig. 3.5b) systems. The results obtained for two CV cycles of monomer electropolymerization we selected for discussion. A resume of the results obtained at the MIP surface for one, two and four CV cycles is shown in Fig. 3.6.

As expected, the AOT thiol deposition caused similar blocking to the redox probe diffusion for both, MIP and NIP, systems. Then, the chip surface was incubated for 2 hours with a BSA solution (C=500 µmol·L^{-1}, in 0.1 mol·L^{-1} PBS at pH 7.4) and a decrease of redox probe signal was observed for the MIP system (see Fig. 3.5b) due to the successful immobilization of BSA at the SAM surface that caused an additional barrier to probe diffusion. By opposition, the peak current intensity remained constant for the NIP surface (see Fig 3.5a) since it was incubated with the pure buffer solution (without template protein). After the electropolymerization (EP) of 3-aminophenol monomer, the decrease of the redox probe signal confirmed the successful deposition of the polymer film in both surfaces. In the last step, the chips were incubated with extraction solution. For the MIP system an increase of the redox probe peak current was observed, meaning that it was easier for the probe molecules to reach the electrode surface, therefore, proving that protein extraction has occurred and the empty binding sites are ready for rebinding. On the other hand, the NIP system presented a decrease of the redox probe signal. This phenomenon was probably due to remaining SDS and/or buffer molecules strongly adsorbed to the electrode surface (or within the polymer matrix) after surface wash that blocked the diffusion of the redox probe to the electrode surface.

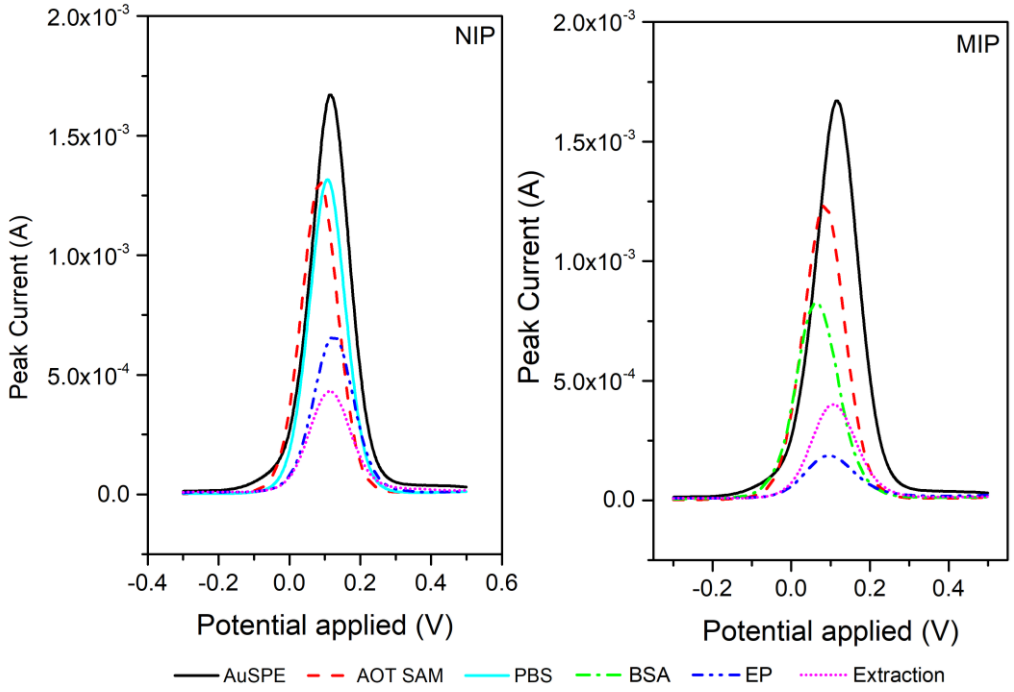

Figure 3.5 – Typical SWVs, obtained in the presence of a 5 mmol·L^{-1} redox probe solution, after step-by-step modification of the AuSPE surface to build the (a) MIP and (b) NIP surfaces. The NIP surface was built by incubation of the sensor surface with PBS (instead of BSA), prior to electropolymerization (EP) process (number of scans: 2, scan rate: 100 mV·s^{-1}).

To summarize the results obtained for the optimization of the thickness of the MIP film, the mean peak current values collected for one, two and four CV cycles during electropolymerization (EP) of the monomer, followed by protein extraction, are presented on Fig. 3.6. As can be seen, due to unexpected circumstances, we couldn't perform the repetition of the experiments for confirmation of the results obtained (error bars are missing for two and four CV cycles).

Even so, based on preliminary results obtained, we can conclude that four CV cycles electropolymerization caused the higher passivation on the electrode surface and limited the amount of protein extracted probably due to the higher thickness of the MIP film, leading to less formation of binding sites at the electrode surface.,

The use of one or two CV cycles for electropolymerization of 3-aminophenol monomer seemed to be more promising for biosensing applications. Therefore, it's possible to theorize that a thinner MIP film, probably matching the protein size, allowed an easier extraction of template protein, and the formation of more binding sites at the electrode surface to achieve higher sensitivity. rebinding studies performed using one CV cycle for monomer electropolymerization were performed in this work.

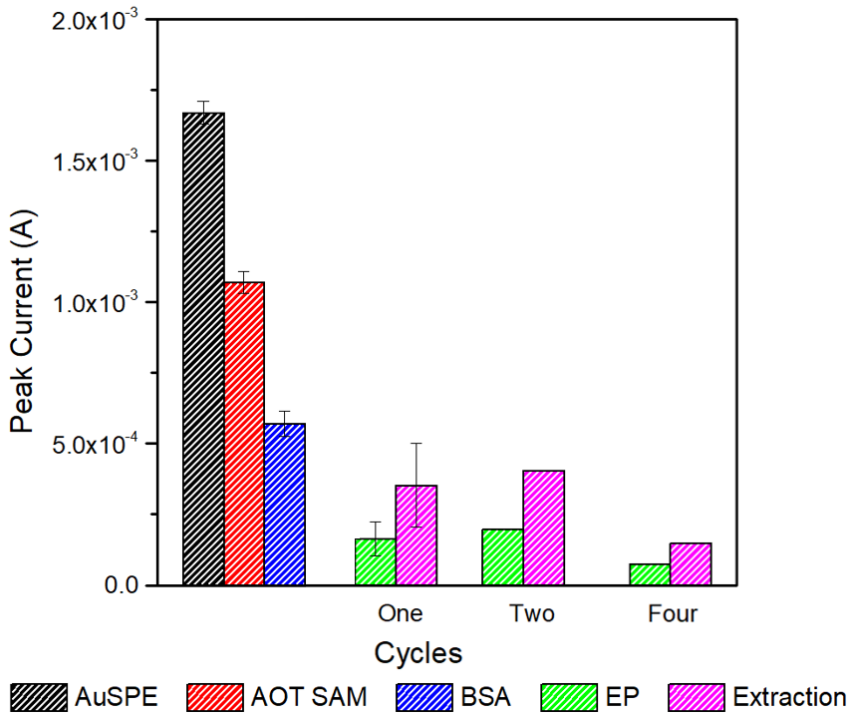

Figure 3.6 - Mean values of SWV peak current intensity, obtained in the presence of a 5 mmol·L^{-1} redox probe solution, obtained for one, two and four CV cycles during (green) electropolymerization (EP) of the monomer, followed by (magenta) protein extraction using an acidic SDS solution. For comparison, the values obtained at the (black) bare AuSPE,(red) SAM/AuSPE, and (blue) BSA/SAM/AuSPE, surfaces were included in the figure . The error bars were obtained from 3 independent repetitions of the experiment.

3.3. Quantification Studies

The extraction of the target protein from the MIP matrix creates a path for the redox couple to pass through, resulting on a readable electrochemical signal [16]. In a similar way, when the pathway is blocked by the rebinding of the target molecule, a decrease of the signal occurs due to the decrease of redox couple concentration at the electrode surface [16].

In order to evaluate the performance of the prepared MIP biosensor for the detection of BSA, protein rebinding studies were performed. After collection of the system baselines, MIP (and NIP) surfaces were incubated for 30 minutes with the binding buffer (0.1 mol·L^{-1} PBS at pH 7.4), containing increasing concentrations of BSA (from 1 nmol·L^{-1} to 100 µmol·L^{-1}), following by surface wash with water. Then, SWV measurements were performed in the presence of the redox probe.

In this work, the collection of the biosensor baseline presented some unexpected difficulties, due to instability of the baselines collected when the chip surface was incubated with PBS only. The typical SWVs collected after repetitive incubation of the sensor surface with PBS, for both, MIP and NIP, systems, is shown in Fig A6.1 (Annex 6). A continuous decrease of the redox probe peak current was observed for both, NIP and MIP, systems, therefore, it is possible to conclude that the baseline instability observed is not related with remaining BSA molecules within the polymer matrix. This phenomenon is probably due to the adsorption and/or interaction of buffer molecules with the electropolymerized film and AuSPE surface, until the equilibrium is reached, and stable baselines are recorded. Thus, in this work a surface stabilization protocol was adopted before the detection studies. The biosensor surface was repetitively incubated with PBS buffer (without BSA) for 5 minutes, followed by SWV measurements, until a reproducible electrochemical response was obtained (baseline stabilization takes about 6 to 7 incubations with PBS, see Fig. A6.1, Annex 6).

After the baseline collection, the sensor surface was incubated with BSA standards to build the calibration curve. The obtained SWVs at the MIP and NIP surfaces are represented on Fig. 3.7.

As can be seen in the figure, a decrease of the redox couple peak current intensity with increasing BSA concentrations was observed for the MIP biosensor, meaning that a successful rebinding of the template protein occurred. However, the results obtained at the NIP surface revealed that non-specific adsorption of protein occurred, also inducing a decrease in the peak current, indicating that this (undesired) type of adsorption plays a relevant contribution for BSA adsorption on the MIP surface.

As stated before, the discussion was based on preliminary data obtained and repetition of the experiments was necessary to increase the confidence of the results obtained.

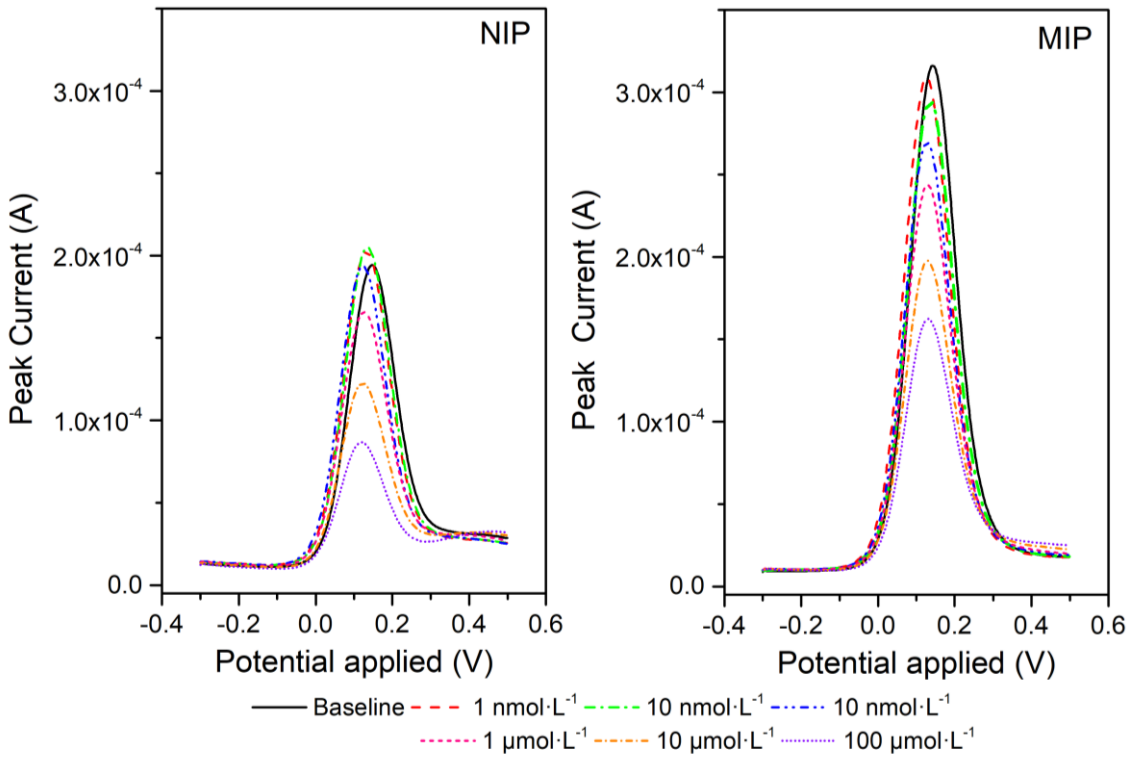

Figure 3.7 – Typical SWVs, obtained in the presence of a 5 mmol·L^{-1} redox probe solution, after incubation of the (left) NIP and (right) MIP surfaces , solutions with increasing concentration of BSA.

The peak current intensity collected from the SWVs was then represented as a function of the logarithm of the BSA concentration, in order to obtain a calibration curve, as shown in Fig. 3.8, for the NIP and MIP surfaces.

From the calibration plots obtained, we can conclude that the MIP biosensor showed a wider working range (and better linearity, R^2=0.981) than the NIP biosensor for concentration values ranging from 0.01 to 100 µmol·L^{-1}. Also, a limit of detection (LOD) bellow 0.01 µmol·L^{-1} was obtained, calculated according to the IUPAC recommendations for ion selective electrodes, where log(C) is used [52]. However, the sensitivity obtained for the NIP film was close to that of the MIP film, meaning that, certainly, the response of the MIP biosensor to BSA was not only due to the imprinted binding sites presented in the MIP film surface, but also through non-specific adsorption of the protein at the sensor surface [13].

To overcome the limitations imposed by the non-specific adsorption, the deposition of a small hydrophilic thiol, such as MCH, after the electropolymerization of the template protein, was considered in this work to block the non-specific adsorption of

the proteins to unoccupied sites at the sensor surface. SPR studies were already performed (see Annex 3), allowing to conclude that BSA had a smaller tendency to adsorb on this hydrophilic thiol, due to the -OH functional groups [53, 54]. Also, a non-specific binding buffer (such as PBS, containing Tween 20) should be used to wash the sensor surface and remove loosely bound protein before SWV measurements.

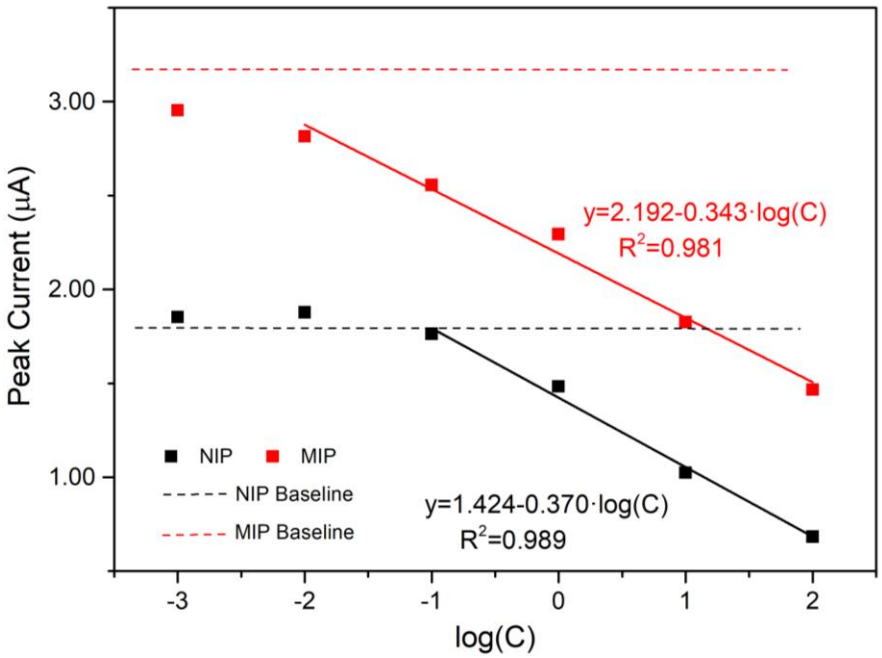

Figure 3.8 – Plot of peak current intensity (Ip) versus the logarithmic concentration of BSA obtained at the (red) MIP and (black) NIP film surfaces. Dashed lines represented in the figure corresponds to baseline values obtained for (black, dash) NIP and (red, dash) MIP.

4. Conclusions and Future Work

4. Conclusions and Future Work

In this work, artificial antibodies were built by using molecular imprinting (MI) technology aiming to develop a new electrochemical sensor device for detection of cancer biomarkers in PoC. Gold screen-printed electrodes (AuSPEs) were used as transducers, since their small size (portability), disposability and low production cost allows their application in clinical diagnosis context

Most of the results presented in this work are relative to the optimization of experimental procedures for preparation of the MIP film at the chip surface. The overall process incorporates the following steps: first, the adsorption of an 8-amino-octane-1-thiol (AOT) self-assembled monolayer (SAM) on the electrode working area allowed the immobilization of template biomolecules at the electrode surface. BSA was used as template protein in these studies. Then, the specific binding sites were created by CV electropolymerization of 3-aminophenol monomer in the presence of the template, giving origin to a poly(3-aminophenol) thin film containing the protein physically entrapped. Finally, target biomolecules were removed from the polymeric matrix and the resulting MIP film recognizes and selectively binds to the template molecules during the rebinding studies.

The preparation of the biosensor and the quantification studies were performed by using electrochemical techniques, namely CV and SWV, in the presence of a suitable reporting system. The signal stability provided by three common redox probes (ferrocyanide/ferricyanide, HAR and FDM) was evaluated at the bare AuSPE surface. These studies allowed to conclude that the most appropriate reporting system was the ferrocyanide/ferricyanide redox couple. SWV technique was selected for the detection studies due to its high sensitivity and rapid time of analysis.

For effective immobilization of template molecules at the electrode surface (and avoid protein denaturation) prior to the electropolymerization process, SAMs of AOT and hexane-1-thiol (HT) were built at the AuSPE surface by incubation of the working electrode with the thiol solution overnight. From the electrochemical and SPR data collected, it was observed that both thiols allowed the immobilization of similar amounts of target protein (difference inferior to 10%) AOT was selected due to its advantages from the experimental point of view. In addition, the SPR results allowed to estimate the optimal concentration of target protein for the imprinting process. The use of an excess BSA concentration of 500 $\mu mol \cdot L^{-1}$ allowed to achieve maximum binding capacity at the SAM surface.

For the preparation of the MIP film, an electropolymerization procedure using CV technique was chosen, allowing simple and fast polymerization procedures (without the need of reaction initiators), and giving origin to stable films at the transducer surface.

After the electropolymerization, the extraction of template protein was performed. From the extraction procedures tested, the incubation of the MIP surface with a SDS solution, prepared in acetate buffer (pH 4.0), provided the most effective approach for protein extraction from the polymer network.

The thickness of the polymer was easily controlled by selecting the number of CV cycles performed during the electropolymerization. One, two and four cycles were tested aiming to study the effect of the film thickness on the biosensor performance. From the preliminary results obtained, the use of one (or two) CV cycles presented the more promising results, since the film obtained by performing four CV cycles seems to be very thick, compromising the template extraction, and consequently, the formation of the specific binding sites at the electrode surface.

Moreover, a preliminary quantification study was performed using a MIP biosensor, prepared using one CV cycle during electropolymerization. Firstly, the MIP surface was stabilized by successive incubations with PBS (without containing BSA) for 5 minutes, followed by SWV measurements until a reproducible response was obtained. Then, rebinding studies were performed by incubating the MIP receptor film with BSA standard solutions in order to build the calibration curve. The MIP biosensor presented a linear response from 0.01 to 100 $\mu mol \cdot L^{-1}$ and a LOD bellow 0.01 $\mu mol \cdot L^{-1}$ was estimated. However, the sensitivity obtained by both surfaces, NIP and MIP, were very similar, meaning that non-specific interactions are affecting the analytical system. However, due to unexpected circumstances, the laboratorial work was interrupted, and the optimization of experimental conditions related to the biosensor preparation was not concluded. Even though that the work done only covers the preliminary steps of the defined plan, fundamental issues related to the optimization of a biosensor for BSA detection were successfully achieved in this work, namely: (i) the electrochemical techniques and the redox probe chosen as reporting system; (ii) the procedures used for template protein immobilization at the electrode surface and for monomer electropolymerization were successfully implemented in this work to increase the biosensor performance and; (iii) the methodology chosen for protein extraction from the polymeric matrix succeeded to achieved the desired results.

Thus, to achieve the goals proposed in this work, the following future work should be performed, namely:

(i) conclude the film thickness optimization studies by performing replicate experiments for two and four CV cycles of electropolymerization process, in order to confirm the preliminary results obtained.

(ii) optimize the surface chemistry procedures, in order to minimize non-specific binding to the MIP surface. Thus, the deposition of a small hydrophilic thiol, such as MCH, after electropolymerization should be included in the MIP preparation protocol aiming to reduce the non-specific adsorption of BSA to unoccupied sites at the sensor surface. Also, a non-specific binding buffer (such as PBS, containing Tween 20) should be used to wash the sensor surface and remove loosely bound protein before SWV measurements.

(iii) after the optimization of the overall process to build the plastic antibodies for detection of BSA, the know-how acquired from the work performed should be transposed for the detection of cancer biomarkers (using these proteins as template biomolecules). The prostate cancer biomarker PSA presents a size and molecular weight similar to BSA, and, therefore, it seems to be a good candidate to apply developed detection approach. Quantification studies of PSA should be performed initially in buffer solution and then, in serum samples spiked with the cancer biomarker.

5. Bibliography

5. Bibliography

1. Phan, H.T., et al., *Investigation of Bovine Serum Albumin (BSA) Attachment onto Self-Assembled Monolayers (SAMs) Using Combinatorial Quartz Crystal Microbalance with Dissipation (QCM-D) and Spectroscopic Ellipsometry (SE).* PLoS One, 2015. **10**(10): p. e0141282.
2. Tothill, I.E., *Biosensors for cancer markers diagnosis.* Semin Cell Dev Biol, 2009. **20**(1): p. 55-62.
3. Thevenot, D.R., et al., *Electrochemical biosensors: recommended definitions and classification.* Biosens Bioelectron, 2001. **16**(1-2): p. 121-31.
4. Whitcombe, M.J., et al., *The rational development of molecularly imprinted polymer-based sensors for protein detection.* Chemical Society Reviews, 2011. **40**(3): p. 1547-1571.
5. Haupt, K., et al., *Molecularly Imprinted Polymers.* Topics in current chemistry, 2011. **325**: p. 1-28.
6. Uzun, L. and A.P.F. Turner, *Molecularly-imprinted polymer sensors: realising their potential.* Biosensors and Bioelectronics, 2016. **76**: p. 131-144.
7. Scheller, F.W., et al., *Molecularly imprinted polymer-based electrochemical sensors for biopolymers.* Current Opinion in Electrochemistry, 2019. **14**: p. 53-59.
8. BelBruno, J.J., *Molecularly Imprinted Polymers.* Chemical Reviews, 2019. **119**(1): p. 94-119.
9. Crapnell, R., et al., *Recent Advances in Electrosynthesized Molecularly Imprinted Polymer Sensing Platforms for Bioanalyte Detection.* Sensors, 2019. **19**(5): p. 1204.
10. Ertürk, G. and B. Mattiasson, *Molecular Imprinting Techniques Used for the Preparation of Biosensors.* Sensors (Basel, Switzerland), 2017. **17**(2): p. 288.
11. Gomes, R., et al., *Sensing CA 15-3 in point-of-care by electropolymerizing O-phenylenediamine (oPDA) on Au-screen printed electrodes.* PLOS ONE, 2018. **13**: p. e0196656.
12. Pacheco, J.G., et al., *Breast cancer biomarker (HER2-ECD) detection using a molecularly imprinted electrochemical sensor.* Sensors and Actuators B: Chemical, 2018. **273**: p. 1008-1014.
13. Ribeiro, J.A., et al., *Disposable electrochemical detection of breast cancer tumour marker CA 15-3 using poly(Toluidine Blue) as imprinted polymer receptor.* Biosens Bioelectron, 2018. **109**: p. 246-254.
14. Sharma, P.S., et al., *Electrochemically synthesized polymers in molecular imprinting for chemical sensing.* Analytical and Bioanalytical Chemistry, 2012. **402**(10): p. 3177-3204.
15. Erdőssy, J., et al., *Enzymatic digestion as a tool for removing proteinaceous templates from molecularly imprinted polymers.* Analytical Methods, 2017. **9**(31): p. 4496-4503.
16. Anzai, J.G., B.; Osa, T., *Electrochemically accelerated adsorption of serum albumin on the surface of platinum and gold electrodes.* Chem Pharm Bull (Tokyo), 1994. **42**(11): p. 2391-3.
17. Guo, B., J. Anzai, and T. Osa, *Adsorption behavior of serum albumin on electrode surfaces and the effects of electrode potential.* Chem Pharm Bull (Tokyo), 1996. **44**(4): p. 800-3.
18. Petrash, S., et al., *Variation in tenacity of protein adsorption on self-assembled monolayers with monolayer order as observed by X-ray reflectivity.* Langmuir, 1997. **13**(7): p. 1881-1883.

19. Love, J.C., et al., *Self-assembled monolayers of thiolates on metals as a form of nanotechnology.* Chem Rev, 2005. **105**(4): p. 1103-69.
20. Fraden, J., *Chemical and Biological Sensors*, in *Handbook of Modern Sensors : Physics, Designs, and Applications*. 2016, Springer International Publishing. p. 645-697.
21. Rebelo, T., et al., *Novel Prostate Specific Antigen plastic antibody designed with charged binding sites for an improved protein binding and its application in a biosensor of potentiometric transduction.* Electrochimica Acta, 2014. **132**.
22. Mollarasouli, F., S. Kurbanoglu, and S.A. Ozkan, *The Role of Electrochemical Immunosensors in Clinical Analysis.* Biosensors, 2019. **9**(3): p. 86.
23. Mohamed, H.M., *Screen-printed disposable electrodes: Pharmaceutical applications and recent developments.* TrAC Trends in Analytical Chemistry, 2016. **82**: p. 1-11.
24. Couto, R.A.S., J.L.F.C. Lima, and M.B. Quinaz, *Recent developments, characteristics and potential applications of screen-printed electrodes in pharmaceutical and biological analysis.* Talanta, 2016. **146**: p. 801-814.
25. Bray, F., et al., *Global cancer statistics 2018: GLOBOCAN estimates of incidence and mortality worldwide for 36 cancers in 185 countries.* CA Cancer J Clin, 2018. **68**(6): p. 394-424.
26. Ferlay, J., et al., *Cancer incidence and mortality patterns in Europe: Estimates for 40 countries and 25 major cancers in 2018.* Eur J Cancer, 2018. **103**: p. 356-387.
27. Mathur, A., et al., *Development of a biosensor for detection of pleural mesothelioma cancer biomarker using surface imprinting.* PLoS One, 2013. **8**(3): p. e57681.
28. Wang, Y., et al., *Molecularly imprinted electrochemical sensing interface based on in-situ-polymerization of amino-functionalized ionic liquid for specific recognition of bovine serum albumin.* Biosensors and Bioelectronics, 2015. **74**: p. 792-798.
29. Ye, L. and K. Mosbach, *Molecular Imprinting: Synthetic Materials As Substitutes for Biological Antibodies and Receptors.* Chemistry of Materials, 2008. **20**(3): p. 859-868.
30. Allen J. Bard , L.R.F., *Electrochemical Methods : Fundamentals and Applications*. 2nd ed. 2001: John Wiley & Sons, Inc.
31. Raheem, Z., *Handbook Of Instrumental Techniques For Analytical Chemistry*, F.A. Settle, Editor. 1997, Simon & Schuster: New Jersey. p. 711-725.
32. Mabbott, G.A., *An Introduction to Cyclic Voltammetry.* Journal of Chemical Education, 1983. **60**(9): p. 697-702.
33. Elgrishi, N., et al., *A Practical Beginner's Guide to Cyclic Voltammetry.* Journal of Chemical Education, 2018. **95**(2): p. 197-206.
34. D. K. Gosser, J., *Cyclic Voltammetry - Simulation and Analysis of Reaction Mechanismc*. 1993, New York: VCH Publishers, Inc. 161.
35. Truhlar, J.H.M.L.C.C.J.C.D.G., *Theoretical Calculation of Reduction Potentials*, in *Organic Electrochemistry - Revised and Expanded*. 2016, CRC Press.
36. Butterworth, A., et al., *SAM Composition and Electrode Roughness Affect Performance of a DNA Biosensor for Antibiotic Resistance.* Biosensors, 2019. **9**(1): p. 22.
37. Fischer, L.M., et al., *Gold cleaning methods for electrochemical detection applications.* Microelectronic Engineering, 2009. **86**(4): p. 1282-1285.
38. Kounaves, S.P., *Voltammetric Techniques*, in *Handbook of Instrumental Techniques for Analytical Chemistry*. 1998, American Chemical Society. p. 709-722.
39. O'Dea, J.J., J. Osteryoung, and R.A. Osteryoung, *Theory of square wave voltammetry for kinetic systems.* Analytical Chemistry, 2002. **53**(4): p. 695-701.

40. Aoki, K., et al., *Reversible square-wave voltammograms independence of electrode geometry.* Journal of Electroanalytical Chemistry and Interfacial Electrochemistry, 1986. **207**(1-2): p. 25-39.
41. Ribeiro, J.A.O., *Caraterização e Otimização de Sensores Eletroquímicos para Aminas Biogénicas*, in *Chemistry and Biochemistry*. 2013, Faculty of Sciences, University of Porto. p. 245.
42. Pereira, C.M.M., *Desenvolvimento de Sensores Voltamétricos com base em Microinterfaces Líquido-líquido Suportadas em Membranas*, in *Chemistry and Biochemistry*. 1997, Faculty of Sciences, University of Porto.
43. Ribeiro, J.A., et al., *Electrochemical detection of cardiac biomarker myoglobin using polyphenol as imprinted polymer receptor.* Anal Chim Acta, 2017. **981**: p. 41-52.
44. Wang, Y., et al., *Voltammetric myoglobin sensor based on a glassy carbon electrode modified with a composite film consisting of carbon nanotubes and a molecularly imprinted polymerized ionic liquid.* Microchimica Acta, 2017. **184**(1): p. 195-202.
45. Li, L., et al., *Aptamer biosensor for label-free square-wave voltammetry detection of angiogenin.* Biosensors and Bioelectronics, 2011. **30**(1): p. 261-266.
46. Snir, E., et al., *A highly sensitive square wave voltammetry based biosensor for kinase activity measurements.* Peptide Science, 2015. **104**(5): p. 515-520.
47. Ribeiro, J., et al., *Electrochemical Characterization of Redox Probes at Gold Screen-Printed Electrodes: Efforts towards Signal Stability.* ChemistrySelect, 2020. **5**: p. 5041-5048.
48. Safety Data Sheet Acessed on 24/09/2020]; Available from: https://www.fishersci.com/store/msds?partNumber=AC215275000&productDescription=1-HEXANETHIOL+96%25&vendorId=VN00032119&countryCode=US&language=en.
49. Armijo, F., et al., *Poly-O-Aminophenol obtained at high potentials by cyclic voltammetry on SNO(2):F electrodes : Application in quantitative determination of ascorbic acid.* Journal of the Chilean Chemical Society, 2009. **54**(2).
50. Reddy, S.M., G. Sette, and Q. Phan, *Electrochemical probing of selective haemoglobin binding in hydrogel-based molecularly imprinted polymers.* Electrochimica Acta, 2011.
51. Barham, A.S., *Electrochemical studies of 3-aminophenol and 3-aminobenzyl Alcohol in Aqueous Solutions at Different pH Values.* Int. J. Electrochem. Sci., 2015. **10**(4): p. 4742-4751.
52. Buck, R.P. and E. Lindner, *Recommendations for nomenclature of ionselective electrodes (IUPAC Recommendations 1994).* Pure and Applied Chemistry, 1994. **66**(12): p. 2527-2536.
53. Ribeiro, J.A., M.G.F. Sales, and C.M. Pereira, *Electrochemistry-assisted surface plasmon resonance detection of miRNA-145 at femtomolar level.* Sensors and Actuators B: Chemical, 2020. **316**: p. 128129.
54. Vaisocherová, H., E. Brynda, and J. Homola, *Functionalizable low-fouling coatings for label-free biosensing in complex biological media: advances and applications.* Anal Bioanal Chem, 2015. **407**(14): p. 3927-53.
55. Homola, J., S.S. Yee, and G. Gauglitz, *Surface plasmon resonance sensors: review.* Sensors and Actuators B-Chemical, 1999. **54**(1-2): p. 3-15.
56. Gupta, B.D. and R.K. Verma, *Surface Plasmon Resonance-Based Fiber Optic Sensors: Principle, Probe Designs, and Some Applications.* Journal of Sensors, 2009. **2009**: p. 1-12.
57. Amendola, V., et al., *Surface plasmon resonance in gold nanoparticles: a review.* J Phys Condens Matter, 2017. **29**(20): p. 203002.
58. Anzai, J.-I., B. Guo, and T. Osa, *Quartz-crystal microbalance and cyclic voltammetric studies of the adsorption behaviour of serum albumin on self-*

assembled thiol monolayers possessing different hydrophobicity and polarity. Bioelectrochemistry and Bioenergetics, 1996. **40**(1): p. 35-40.

Annex 1

ChemistrySelect | Full Papers doi.org/10.1002/slct.202001411 | Chemistry Europe European Chemical Societies Publishing

Electro, Physical & Theoretical Chemistry

Electrochemical Characterization of Redox Probes at Gold Screen-Printed Electrodes: Efforts towards Signal Stability

José A. Ribeiro,* Elisa Silva, Patrícia S. Moreira, and Carlos M. Pereira*[a]

In this work, three universally used redox probes in amperometric biosensing devices, $[Fe(CN)_6]^{3-}$/$[Fe(CN)_6]^{4-}$, $Ru[(NH_3)_6]^{3+}$, and ferrocenedimethanol (FDM), were selected to evaluate the stability of electrochemical signals provide by the reporting systems. Studies were carried out at disposable gold screen-printed electrode (AuSPE) biosensing platforms, commonly used for screening chemical and biological relevant biomolecules. Firstly, electrochemical combined-surface plasmon resonance (eSPR) studies were performed to evaluated adsorption reversibility and/or formation of redox probe complexes at the bare gold surface when routinely used electrochemical techniques, namely cyclic voltammetry (CV) and square-wave voltammetry (SWV), are recorded. Then, the results obtained were compared with those obtained at the AuSPE under the same electrochemical conditions. Based on our findings, best experimental conditions, including the type of electrochemical technique used, are speculated for each reporting system in order to improve the analytical signal stability.

Finally, a methodology based on SWV technique was applied to modified electrodes to provide a simple and easy tool to ensure diffusion controlled permeability of probes thorough the films to electrode surface.

Introduction

Electrochemical methods are a powerful approach for the sensitive screening of clinically and environmental relevant biomolecules, including proteins and nucleic acids.[1] Biorecognition elements currently used in the construction of sensor platforms are very diverse and includes antibodies, enzymes, nucleic acids, aptamers, among others.[2,3] Also, the use of molecularly imprinted polymers (MIP) to mimic the binding sites of target biomolecule is currently a widespread approach to develop new biosensing devices with high selectivity toward a particular analyte.[4–6] Moreover, the use of (low cost) disposable screen-printed electrodes (SPE) is very attractive for electroanalysis since it offers easy handling, low sample volume requirement and possibility of mass production and miniaturization of detection devices (portability), which can be particularly useful for the fast, simple and sensitive determination of environmental pollutants,[7] pathogens[8] or biological markers,[2–4] in Point-of-Care (PoC).

Most of the electrochemical approaches with amperometric readout employed for detection of non-redox-active biomolecules are based on the permeability of a selected diffusional redox probe through the thin films covering the electrode surface.[6] Thus, while SPR, QCM, among other techniques, can be easily applied, the successful application of amperometric devices depend strongly on several experimental parameters, such as composition and ionic strength of electrolyte and redox probes used. In this context, the redox probe used has to fulfill a number of requirements, including stability of the oxidized/reduced states, good biocompatibility and, more importantly, no irreversible deposition or corrosion of the electrodes should occur.[9]

In our laboratory, a ferrocyanide/ferricyanide solution was selected to monitor the surface modification of a gold SPE (AuSPE) and, sometimes, serious experimental problems were observed. Namely, when electrochemical measurements in the presence of redox probe solution were performed at bare chips prior to modification, the subsequent electropolymerization of thionine at the electrode surface was compromised when compared with gold chips without previous incubation with ferrocyanide/ferricyanide solution (see Figure S1, SI). After a careful search through the literature dealing with the topic, we found out some recent works reporting some drawbacks associated to the use of the redox probe. EIS studies suggested great care or recommended not to use ferrocyanide/ferricyanide redox couple in combination with gold electrodes for several reasons, namely: (1) interaction of ferrocyanides with gold leads to the formation of polymeric complexes at the electrode surface;[10,11] (2) the presence of unbound cyanide ions (CN^-), which are released from the ferrocyanide/ferricyanide redox probe due to decomposition by UV irradiation, can cause permanent damage of gold surface;[11,12] (3) chloride ions composing the PBS may adsorb onto the gold electrode and alter the kinetics of the redox system[13] and; (4) instability of thiol monolayers at the gold surface due to reaction with $[Fe(CN)_6]^{3-/4-}$ redox couple.[14] In addition, some limitations were also associated to SPEs,[3] such as: (1) possible damage of the electrode surface when very harsh conditions are used (like highly acidic/basic solutions, chaotropic agents, proteases, etc.);

[a] Dr. J. A. Ribeiro, E. Silva, P. S. Moreira, Prof. C. M. Pereira
CIQUP/Department of Chemistry and Biochemistry, Faculty of Sciences of University of Porto, Rua do Campo Alegre 687, s/n, Porto 4169-007, Portugal
E-mail: jose.ribeiro@fc.up.pt
cmpereir@fc.up.pt

Supporting information for this article is available on the WWW under https://doi.org/10.1002/slct.202001411

© 2020 Wiley-VCH Verlag GmbH & Co. KGaA, Weinheim

ChemistrySelect | Full Papers doi.org/10.1002/slct.202001411 | Chemistry Europe European Chemical Societies Publishing

(2) several assays need to be performed to obtain reliable data (lack of stability) and; (3) experienced personnel is often required to conduct the measurements to avoid misinterpretation of data collected.

Although some concerns about the use of ferrocyanide/ferricyanide redox species when performing ESI technique at gold surfaces have been expressed by some research groups, very little is known about the behavior of the redox couple or other redox probes commonly used by electrochemists (such as hexaammineruthenium), when other electrochemical techniques are used for analytical purposes, such as cyclic voltammetry (CV) or pulse techniques. Thus, in this work, efforts were made to bring new insights about stability of redox probe signals, contributing to avoid erroneous results, and aiming to increase the repeatability of the measurements. Three redox probes were tested, the routinely used ferrocyanide/ferricyanide redox couple, the positively charged hexaammineruthenium (HAR) and the water soluble ferrocene dimethanol (FDM). Due to the distinctive features and widespread use in biosensing studies, AuSPEs were used as sensor platforms in this work. The redox probe profiles and possible biosensing applications are shown in Scheme 1.

To achieve our goal, electrochemistry combined-SPR (eSPR) measurements were conducted in first place to study the effect of incubation times and type of electrochemical techniques performed on probe adsorption reversibility and/or formation of secondary products at the bare gold surface. CV and square wave voltammetry (SWV) were selected for the studies and two electrochemical conditions were tested: (1) three CV cycles were recorded followed by a SWV measurement (CV + SWV) or (2) a single SWV voltammogram was recorded (without previous CV cycles). Then, the stability of electrochemical redox probe signals was evaluated and compared for three redox probes studied by performing repetitive electrochemical measurements over the same bare AuSPE in order to achieve best experimental conditions for stable electrochemical response.

Results and Discussion

It is known that several factors can influence the performance and stability of amperometric biosensors,[13] such as appropriate electrode surface cleaning protocols, electrolytes and redox probes used, incubation times in redox couple solution, among others. However, little is known about the adsorption behavior of these substances in gold chips when routinely electrochemical techniques (such as CV or pulse techniques) are used during the construction of the sensor platforms and detection. Thus, we have performed eSPR investigations to study the adsorption phenomena of the redox probes $[Fe(CN)6]^{3-/4-}$, $[Ru(NH_3)]^{3+}$ and FDM at the gold SPR substrates. The redox probes

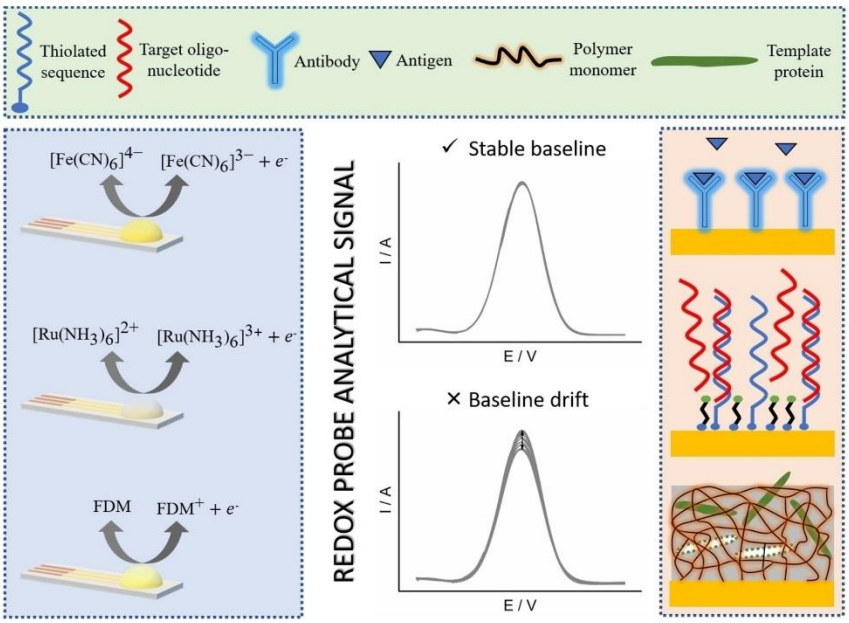

Scheme 1. Redox probes studied in this work at the AuSPE surface and possible applications in amperometric detection of chemical and biological relevant biomolecules.

© 2020 Wiley-VCH Verlag GmbH & Co. KGaA, Weinheim

ChemistrySelect | Full Papers doi.org/10.1002/slct.202001411 | Chemistry Europe European Chemical Societies Publishing

were dissolved in 0.1 mol L^{-1} Na_2SO_4, a chloride ion free electrolyte, at a concentration level of 5 mmol L^{-1}, typically used in biosensing systems. Routinely used electrochemical techniques CV and SWV were selected for the studies.

Electrochemistry combined-SPR (eSPR) measurements at the gold SPR surface

In an attempt to study the adsorption behavior of redox probes at the electrode surface and its equilibrium dynamics with incubation medium molecules, we have performed 10 successive injections of redox probe solution into the measuring channel and electrochemical measurements at bare gold SPR surface were performed. The real-time SPR monitoring of adsorption of redox probes studied is shown in Figure 1. The effect of the type and number of electrochemical measurements performed over the same gold surface was evaluated by performing (1) a single SWV measurement or (2) three CV cycles followed by a SWV measurement (CV + SWV). For comparison, the SPR response obtained when (3) no electrochemical measurements were performed was also recorded. The incubation time was the same for the three electrochemical conditions tested.

Based on the sensorgrams shown in Figure 1A, we can infer that HCF has residual adsorption on the gold surface under the electrochemical conditions used. Even after performing 10 repeated electrochemical measurements (SWV only or CV + SWV), a small shift of the SPR angle is observed (see Figure 1D). These results are somewhat surprising since studies reported in the literature shows irreversible adsorption and formation of HCF complexes at the gold surface.[10,11] Probably this process is more pronounced for techniques requiring long incubation times, such as ESI, and is not so notorious for fast CV and SWV recording (SWV takes only few seconds and CV + SWV takes about 1–2 minutes).

A very distinct SPR response was observed for HAR (see Figure 1B) and FDM (see Figure 1C) redox probes. The simple contact of the electrode surface with probe solution (no electrochemical process occurs) induces some irreversible adsorption of probe molecules that remains nearly constant

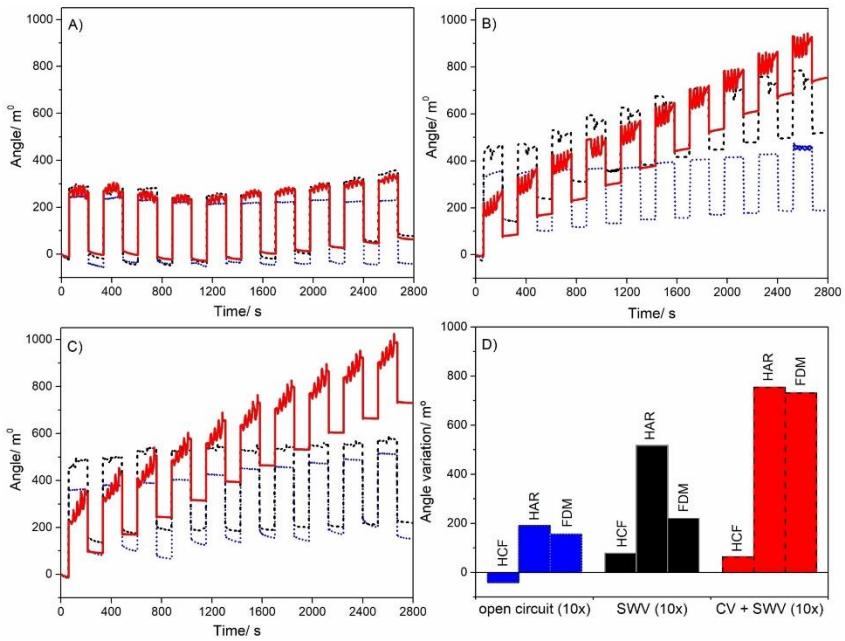

Figure 1. Real-time SPR monitoring of the interaction between redox probes A) $[Fe(CN)_6]^{3-/4-}$, B) $[Ru(NH_3)_6]^{3+}$ and C) FDM with SPR gold substrates. The baseline was collected in 10 mmol L^{-1} PBS, pH 7.4, for 60 s; Then, combined electrochemical measurements and SPR detection were performed after injection of 5 mmol L^{-1} redox probe solution into the measuring channel. After equilibration at open circuit, SWV (dashed lines, black) or 3 cycles CV followed by SWV (solid lines, red) were recorded between −0.3 – 0.5 V (*vs.* Ag/AgCl) for $[Fe(CN)_6]^{3-/4-}$ and FDM and between −0.65 – 0 V (*vs.* Ag/AgCl) for $[Ru(NH_3)_6]^{3+}$. For comparison, the SPR response obtained when (dotted lines, blue) no electrochemical measurements were performed is also shown in the figure. Finally, the surface was washed with PBS for 120 s (return to baseline). The procedure was repeated 10 times. (D) Graphical representation of the total angle variation obtained after 10 baselines collection under the different electrochemical conditions tested.

© 2020 Wiley-VCH Verlag GmbH & Co. KGaA, Weinheim

ChemistrySelect
Full Papers
doi.org/10.1002/slct.202001411
Chemistry Europe
European Chemical Societies Publishing

during the eSPR investigation. In addition, it seems that repeated oxidation and reduction cycles (CV + SWV) favors the continuous accumulation of probe molecules, or related surface-complexes, at the electrode surface. A total SPR angle variation of 730 and 760 m° was obtained for FDM and HAR (see Figure 1D), respectively, meaning that a huge amount of material resulting from electrochemical processes is irreversibly deposited at the gold surface. However, lower overall angle shifts were obtained when SWV only is recorded. This is probably due to the less extension of the electrochemical reactions suffered by the redox probes (one scan per SWV). Interestingly, no appreciable angle variation was obtained for the FDM redox probe after performing repeated SWVs relatively to the reference system, where no electrochemical measurements were performed (see Figure 1D).

Since the SPR response was combined with electrochemical measurements, the stability and reproducibility of the redox probe electrochemical response was evaluated under the established conditions. Figure 2 depicts the redox probe peak current ($I_{peak(SWV)}$) variation obtained for the 10 SWV voltammograms recorded at the gold SPR substrates.

After analysis of the voltammetric data collected during the eSPR measurements, the analytical signal stability was correlated with the probe adsorption reversibility at the gold surface. In this context, from the three reporting systems tested, HCF showed the higher signal variability (see Figure 2A). This result was not expected since no appreciable SPR angle variation was observed for the redox couple under the electrochemical conditions tested, which, in principle, should provide high reliable data. The highest $I_{peak(SWV)}$ variation (of about 129% of the starting value) was obtained when SWV technique only was performed and RSD values greater than 5% were obtained when SWV, combined or not with CV, was performed, which indicates poor signal reproducibility.

For HAR (see Figure 2B) and FDM (see Figure 2C), the electrochemical signal tends to decrease as the number of repeated electrochemical measurements over the same bare gold surface increases (CV + SWV) till maximum signal variation is reached (87% for HAR and 90% for FDM). The $I_{peak(SWV)}$ continuous decrease after the 3th and 6th injection of HAR and FDM probe solution, respectively, into the measuring channel. Taking into account the eSPR studies, this effect seems to be related to the high accumulation of redox probe species at the

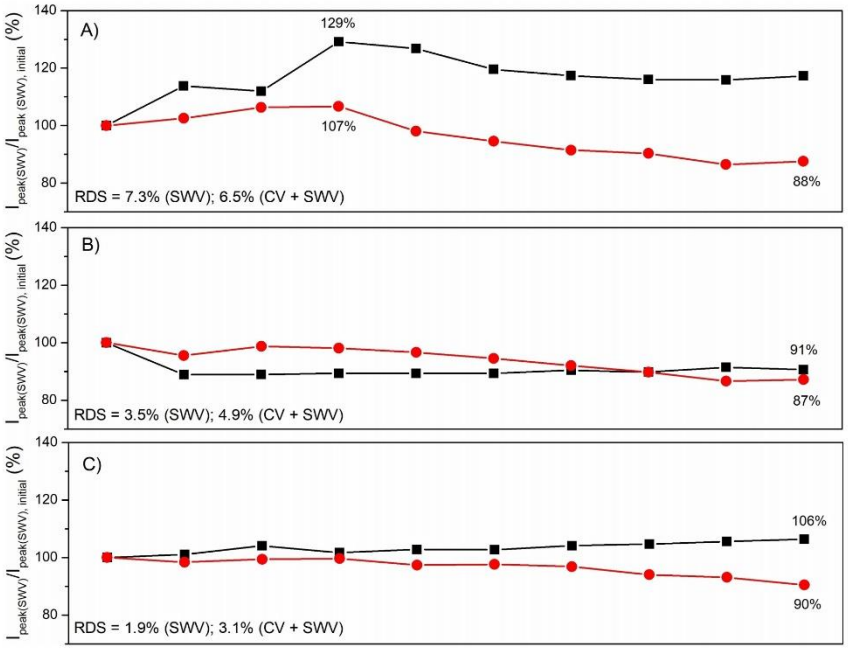

Figure 2. Graphical representation of the stability of the redox probe peak current obtained from SWV voltammograms ($I_{peak(SWV)}$) collected over the 10 repeated electrochemical measurements at the bare gold SPR surface, using SWV technique (■, black) and combined CV + SWV techniques (●, red), for the redox probes A) $[Fe(CN)_6]^{3-/4-}$, B) $[Ru(NH_3)_6]^{3+}$ and C) FDM. SWV voltammograms collected under the specified electrochemical conditions are represented in Figure S2 and Figure S3, SI.

© 2020 Wiley-VCH Verlag GmbH & Co. KGaA, Weinheim

ChemistrySelect
Full Papers
doi.org/10.1002/slct.202001411
Chemistry Europe
European Chemical Societies Publishing

electrode surface resulting from repeated CV + SWV measurements, leading to higher peak current variability (RSD values of 4.9% and 3.1% were estimated for HAR and FDM, respectively).

Under electrochemical conditions of single SWV measurement, no clear tendency of the analytical signal was observed and higher stability was achieved for both HAR and FDM redox probes. Lower signal variations (of 9% and 6% for HAR and FDM, respectively) and RSD values (of 3.5% and 1.9% for HAR and FDM, respectively) were obtained relatively to combined CV + SWV techniques. Between the two redox probes, FDM showed higher electrochemical signal stability than HAR, probably due to the more pronounced HAR probe components adsorption on the gold surface when SWV only was recorded (see Figure 1D).

Electrochemical measurements at the AuSPEs

Redox probe analytical signal stability is a key factor to achieve reproducible results. Although decrease of peak current intensity after incubation steps with PBS was reported,[13] inducing false sensitivities, this effect is probably related to chloride ions composing the buffer solution that adsorbs on gold surface. In our experiments, a chloride free buffer was used to avoid signal drifts merely associated to incubation steps, meaning that any apparent signal tendency should be related to the irreversible deposition of redox probe molecules or related compounds at the electrode surface.

The stability of redox probe signals at bare AuSPEs was studied by SWV, combined or not with CV technique (CV+ SWV). A series of 10 repeated electrochemical measurements were performed at the same bare chip surface followed by surface incubation with PBS for 2 min. The electrode surface was washed with pure water after each surface incubation step. Based on SWV voltammograms collected under the electrochemical conditions tested, the peak current ($I_{peak(SWV)}$) changes relatively to initial value ($I_{peak(SWV),\ initial}$) obtained before surface incubation with PBS, is show in Figure 3, for the three probes tested.

Higher signal stability was obtained for the HCF redox couple at the gold ink surface relatively to the thin gold films prepared by chemical vapor deposition used in eSPR. Besides, a random change of the SWV peak current was observed when single SWV or combined (CV + SWV) measurements are performed at the AuSPE (see Figure 3A). These results are

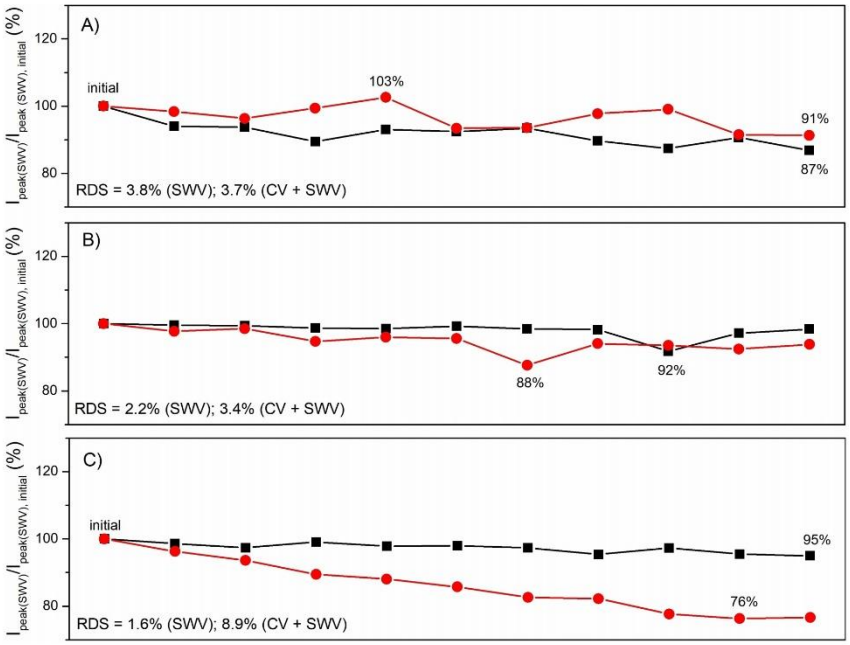

Figure 3. Graphical representation of the stability of the redox probe SWV peak current ($I_{peak\ (SWV)}$) over the 10 repeated electrochemical measurements performed over the same bare AuSPE surface, using SWV technique (■, black) and combined CV + SWV techniques (●, red), for the redox probes A) $[Fe(CN)_6]^{3-/4-}$, B) $[Ru(NH_3)_6]^{3+}$ and C) FDM. SWV voltammograms collected under the specified electrochemical conditions are represented in Figure S4 and Figure S5, SI.

© 2020 Wiley-VCH Verlag GmbH & Co. KGaA, Weinheim

ChemistrySelect | Full Papers doi.org/10.1002/slct.202001411 | Chemistry Europe European Chemical Societies Publishing

consistent with the eSPR experiments, where no significant irreversible adsorption of redox probe solution components was registered for both electrochemical conditions tested. Maximum $I_{peak(SWV)}$ variations relatively to initial value obtained were of 87% when SWV technique only was used and between 103% and 91% for combined CV + SWV. Similar RSD values (of 3.8% and 3.7%) were obtained for both electrochemical conditions tested.

Relatively to HAR (see Figure 3B), although a continuous decrease of $I_{peak(SWV)}$ was observed in the eSPR measurements when repetitive CV + SWV was performed, no tendency was observed in the $I_{peak(SWV)}$ variation at the gold chips under both electrochemical conditions tested. Moreover, maximum $I_{peak(SWV)}$ variations of 12% and 8% and RSD values of 3.4% and 2.2% were obtained, after performing single SWV measurement and combined CV + SWV, respectively, revealing an apparent stable electrochemical response at the AuSPE. Moreover, hexaammineruthenium (III) was recently reported as a viable alternative redox probe to replace HCF in ESI studies for detection of biomolecules at gold SPEs.[9] However, high SWV potential drift during the assay was observed for this probe (see Figure S4 and Figure S5, SI). This effect is probably related to the chloride ions present in the probe solution, after dissolving the HAR salt, which are supposed to interact with the screen-printed silver pseudo-reference electrode causing the measured potential to change.[15] It's important to notice that no potential drift was observed during the eSPR measurements where an Ag/AgCl (saturated KCl) wire is used as reference electrode. Other electrolyte solutions, such as PBS, can be tested to minimized or overcome the potential drift.

For FDM (see Figure 3C), the combination of CV + SWV techniques clearly affects signal stability at the electrode surface and a continuous decrease of peak current is observed after repetitive measurements. This effect was already observed in the eSPR measurements, indicating electrode surface fouling on continuous use by products from redox processes occurring during CV. This process is more notorious at AuSPE probably due to some effect from the surface roughness or ink composition comparing to the smooth gold SPR surface, leading to less reversible behavior and higher accumulation of FDM (or related species) at the chip surface. Maximum $I_{peak(SWV)}$ decrease of 76% relatively to initial peak current while a RSD value of 8.9% were obtained, confirming the degradation of the electrochemical response when repetitive CV + SWV are recorded over the same electrode surface. By opposition, when single SWV measurement is performed, the FDM redox probe showed the higher signal stability over the entire measurement procedure. Maximum $I_{peak(SWV)}$ variation of 5% and a RSD value of only 1.6% were estimated. Moreover, the water soluble ferrocene FDM can be a very interesting alternative to the more routinely used redox probes. His standard reversible potential is similar to the HCF, and much higher than the HAR,[16] and no chloride ions compose the probe solution. Besides, FDM carries no charge, meaning that it can easily permeate through highly charged layers at the electrode surface (such as proteins, antibodies, polymers, nucleic acids, etc.) without suffering electrostatic interactions.

Finally, all redox probes provided adequate levels of reproducibility of generated electrochemical signal at AuSPEs, even when CV was performed before SWV, with the exception of FDM, where repetitive CV cycles should avoid to maintain signal stability.

Redox probe behavior at modified AuSPEs

In this work, simple and rapid studies, using the SWV technique, were performed in order to gather information about the redox probe behavior at functionalized gold surfaces. In short, the methodology consisted in altering the SWV amplitude at a fixed frequency of the potential modulation (scan rate of the voltammetric experiment is maintained constant).[17] For a dissolved redox couple at a planar electrode, if quasireversible electrode reaction occurs, a distinct maximum is predicted for the dependence of the amplitude-normalized net SWV peak current ($I_{peak(SWV)}/\Delta E_{SWV}$) versus the SWV amplitude (ΔE_{SWV}) while a monotonous decrease of ($I_{peak(SWV)}/\Delta E_{SWV}$) *vs.* ΔE_{SWV} is observed for full reversibility reaction.[17] The studies were performed before and after gold surface modification with typical thin films covering the electrode surface, such as thiolated SAMs or polymers, in order to test the applicability of the kinetic methodology. SAMs at gold surface are typically used as basis to attach target biomolecules (such as proteins) or biological receptors (antibodies, enzyme, nucleic acids, etc.) while synthetic polymers obtained by polymerization are used to create MIP receptor surfaces for biosensing.

The variation of the amplitude-normalized peak current in SWV ($I_{peak(SWV)}/\Delta E_{SWV}$) with the pulse amplitude (ΔE_{SWV}) is shown in Figure 4 for the three redox probes studied. As can be seen, the curves obtained at bare AuSPE shows a continuous decrease of the $I_{peak(SWV)}/\Delta E_{SWV}$ versus ΔE_{SWV} for the reporting systems under study. Moreover, SWV measurements were also performed at the polycrystalline gold electrode surface, which has a more stable and reproducible electrochemical response, in order to compare the results obtained from the common kinetic methodology (see Figure S9). The results obtained at polycrystalline gold surface are consistent with the obtained at gold ink surface, indicating full reversible diffusion-controlled reaction of the redox probes tested at the gold electrode surface.

Although thiol instability, especially in the presence of $[Fe(CN)_6]^{3-/4-}$, was reported in the literature,[14] our results indicate a fully reversible diffusion controlled redox process at the AOT modified surface for the three redox probes tested and no signs of unstable modification was observed under the experimental conditions tested. Moreover, after electropolymerization of non-conductive poly(3-aminophenol) at the AuSPE surface a reversible-diffusion limited process was observed for the three redox probes tested. Thus, in principle, AOT/AuSPE and poly(3-amiphenol)/AuSPE modified electrodes are suitable for biosensing purposes using the reporting systems tested.

For the conducting poly(thionine) film on the AuSPE, the redox makers' species showed different diffusivities. A distinct kinetic curve profile was observed for HCF relatively to HAR and FDM. As can be seen in Figure 4A, a well-defined maximum

 © 2020 Wiley-VCH Verlag GmbH & Co. KGaA, Weinheim

ChemistrySelect
Full Papers
doi.org/10.1002/slct.202001411
Chemistry Europe
European Chemical Societies Publishing

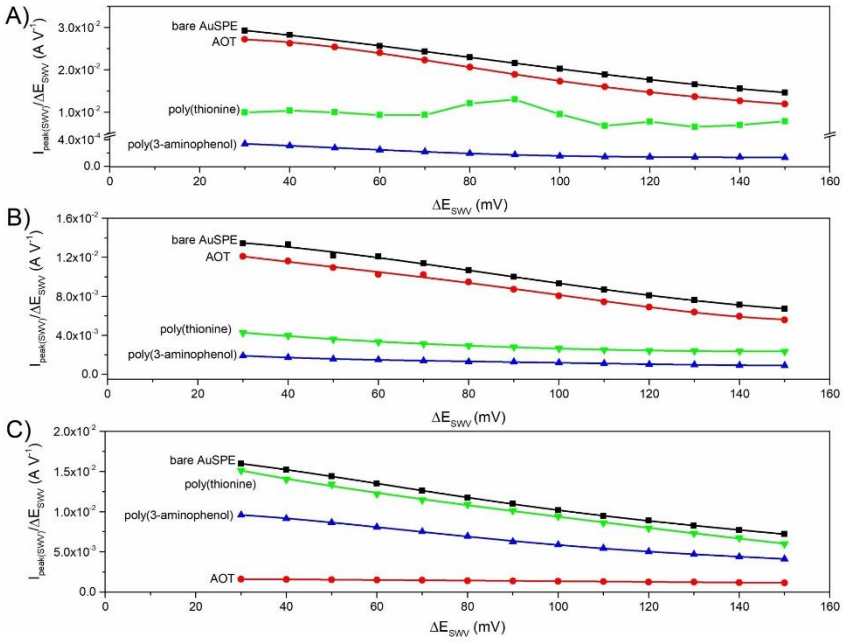

Figure 4. Variation of the amplitude-normalized peak current in SWV ($I_{peak(SWV)}/\Delta E_{SWV}$) with the pulse amplitude (ΔE_{SWV}) for the redox probes A) $[Fe(CN)_6]^{3-/4-}$, B) $[Ru(NH_3)_6]^{3+}$ and C) FDM. Representative SWV voltammograms at bare AuSPE for different pulse amplitude values are represented in Figs. S6 – S8, SI.

is observed between amplitudes 70 and 110 mV indicating that electron process is not fully reversible. Probably, electrostatic interaction between small anions of $[Fe(CN)_6]^{3-/4-}$ and the positively charged film caused rapid adsorption of the probe molecules within the polymeric matrix to maintain the overall charge neutrality.[18] Thus, the use of HCF as redox probe when the sensor surface is composed by a polymer layer of thionine can compromise detection ability. By opposition, kinetic curves obtained with HAR or FDM redox probes showed a continuous decrease corresponding to reversible electrode reactions and diffusion of redox probes through the polymer film to electrode surface, making them suitable for biosensing studies using poly (thionine).

Although the electrode surface modifications shown are merely representative, the authors think that the methodology based on SWV technique can provide a simple and rapid tool to support the choice of the well-behaved reporting system in order to obtain stable and reliable results when developing new amperometric devices.

Conclusion

In this work, concerns related to amperometric biosensing of non-electroactive biomolecules were considered, namely, the lack of stability of redox probe signals at gold SPEs under certain conditions, which can give origin to erroneous results. Thus, in order to evaluate the drift impact caused by the type electrochemical technique record, eSPR and electrochemical investigations were performed using SWV or combined CV + SWV techniques. Three routinely used reporting systems, HCF, HAR and FDM, were tested.

The SPR results obtained indicate that, for some redox probes, detection stability can be affected by repetitive electrochemical processes, which promotes the continuous surface accumulation of redox probe species at the electrode surface. This effect was particularly evident for HAR and FDM. By opposition, no significant irreversible deposition of HCF at the gold surface was observed under the electrochemical conditions tested.

Acceptable signal variations were obtained during electrochemical investigations conducted at AuSPEs when repetitive single SWV or combined CV + SWV measurements were recorded, except for FDM, where repetitive CVs should be avoided in order to obtain stable blank response. Moreover, more stable electrochemical response was obtained for HAR and FDM when single SWV measurement is recorded, which, in principle should provide more reliable data.

© 2020 Wiley-VCH Verlag GmbH & Co. KGaA, Weinheim

ChemistrySelect | Full Papers doi.org/10.1002/slct.202001411 | Chemistry Europe European Chemical Societies Publishing

Taking into account the results obtained this work and recommendations found in literature, the optimization of experimental conditions seems to be critical to overcome the lack stability posed by redox probes at AuSPEs, namely: (1) relatively low concentration of redox probe and chloride free electrolyte solutions should be prepared and stored in absence of daylight; (2) minimize multiple measurements (and multiple incubations) at the same sensor surface; (3) select appropriate techniques to minimize detection times. In fact, SWV technique seems to be a very good option since it offers rapid measuring time (low incubation times), well-defined analytical peaks and high detection sensitivity; (4) keep the potential limits as small as possible during the electrochemical measurements. Also, based on our findings, we have great concerns about reusability of AuSPEs unless very effective cleaning of redox probe species from the electrode surface can be achieved.

Finally, a simple and rapid methodology based on SWV technique was tested at functionalized AuSPEs in order to ensure full reversible electron reaction and diffusion-controlled permeation of the probe molecules through the films to the electrode surface.

Supporting Information Summary

Supporting Information includes the complete Experimental Section, the voltammograms of thionine electropolymerization, the SWVs collected during the eSPR studies and the variation of the amplitude-normalized peak current in SWV with the pulse amplitude, obtained at the polycrystalline gold electrode surface.

Acknowledgements

This research had the financial support of FCT (Fundação para a Ciência e Tecnologia) and co-financed by the European Union (FEDER funds) under the Partnership Agreement PT2020, Research Grant Pest-C/QUI/UIDB/00081/2020 (CIQUP). J.A. Ribeiro (ref. SFRH/BPD/105395/2014) and C.M. Pereira (ref. SFRH/BSAB/150320/2019) acknowledge FCT under the QREN – POPH – Advanced Training, subsidized by European Union and national MEC funds.

Conflict of Interest

The authors declare no conflict of interest.

Keywords: amperometric · biosensors · gold · redox probe · screen-printed electrode (SPE)

[1] M. Labib, E. H. Sargent, S. O. Kelley, *Chem. Rev.* **2016**, *116*, 9001–9090; S. N. Topkaya, M. Azimzadeh, M. Ozsoz, *Electroanalysis* **2016**, *28*, 1402–1419.
[2] F. S. Felix, L. Angnes, *Biosens. Bioelectron.* **2018**, *102*, 470–478.
[3] K. K. Mistry, K. Layek, A. Mahapatra, C. RoyChaudhuri, H. Saha, *Analyst* **2014**, *139*, 2289–2311.
[4] J. J. BelBruno, *Chem. Rev.* **2019**, *119*, 94–119.
[5] a) L. Uzun, A. P. F. Turner, *Biosens. Bioelectron.* **2016**, *76*, 131–144; b) A. A. Lahcen, A. Amine, *Electroanalysis* **2019**, *31*, 188–201.
[6] F. W. Scheller, X. Zhang, A. Yarman, U. Wollenberger, R. E. Gyurcsányi, *Curr. Opin. Electrochem.* **2019**, *14*, 53–59.
[7] M. Li, Y.-T. Li, D.-W. Li, Y.-T. Long, *Anal. Chim. Acta* **2012**, *734*, 31–44.
[8] P. Skládal, *Curr. Opin. Electrochem.* **2019**, *14*, 66–70.
[9] J. D. Schrattenecker, R. Heer, E. Melnik, T. Maier, G. Fafilek, R. Hainberger, *Biosens. Bioelectron.* **2019**, *127*, 25–30.
[10] A. Bogomolova, E. Komarova, K. Reber, T. Gerasimov, O. Yavuz, S. Bhatt, M. Aldissi, *Anal. Chem.* **2009**, *81*, 3944–3949.
[11] J. Lazar, C. Schnelting, E. Slavcheva, U. Schnakenberg, *Anal. Chem.* **2016**, *88*, 682–687.
[12] S. Vogt, Q. Su, C. Gutiérrez-Sánchez, G. Nöll, *Anal. Chem.* **2016**, *88*, 4383–4390.
[13] B. L. Garrote, A. Santos, P. R. Bueno, *ACS Sens.* **2019**, *4*, 2216–2227.
[14] R. B. Channon, Y. Yang, K. M. Feibelman, B. J. Geiss, D. S. Dandy, C. S. Henry, *Anal. Chem.* **2018**, *90*, 7777–7783.
[15] U. Guth, F. Gerlach, M. Decker, W. Oelßner, W. Vonau, *J. Solid State Electrochem.* **2009**, *13*, 27–39.
[16] A. K. Neufeld, A. P. O'Mullane, *J. Solid State Electrochem.* **2006**, *10*, 808–816.
[17] V. Mirceski, E. Laborda, D. Guziejewski, R. G. Compton, *Anal. Chem.* **2013**, *85*, 5586–5594, J. M. Olmos, A. Molina, E. Laborda, F. Martínez-Ortiz, *Electrochim. Acta* **2015**, *176*, 1044–1053.
[18] T.-H. Le, Y. Kim, H. Yoon, *Polymers* **2017**, *9*, 150.

Submitted: April 6, 2020
Accepted: April 21, 2020

 © 2020 Wiley-VCH Verlag GmbH & Co. KGaA, Weinheim

FULL PAPERS

Redox probes studied in this work, at the gold screen-printed electrode (SPE) surface, were: $[Fe(CN)_6]^{3-}$/$[Fe(CN)_6]^{4-}$ redox couple, $Ru[(NH_3)_6]^{3+}$ and ferrocenedimethanol (FDM). Their possible application in amperometric detection of chemical and biological relevant biomolecules is also shown. Electrochemical signal stability provided by each reporting system was evaluated when routinely used electrochemical techniques, namely cyclic voltammetry (CV) and square-wave voltammetry (SWV), are recorded.

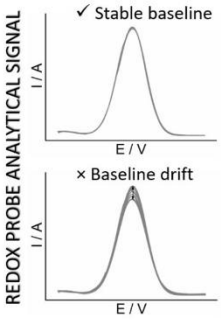

Dr. J. A. Ribeiro, E. Silva, P. S. Moreira, Prof. C. M. Pereira**

ChemistrySelect

Supporting Information

Electrochemical Characterization of Redox Probes at Gold Screen-Printed Electrodes: Efforts towards Signal Stability

José A. Ribeiro,* Elisa Silva, Patrícia S. Moreira, and Carlos M. Pereira*

Supporting Information (SI)

Experimental Section

Chemicals and solutions

The chemicals used throughout this work were: 8-amino-1-octanethiol (AOT, Dojindo Laboratories), 3-aminophenol (98%, Sigma-Aldrich), thionine (Alfa Aesar), potassium ferricyanide ($K_3[Fe(CN)_6]$, ≥99.0%, Fluka), potassium ferrocyanide ($K_4[Fe(CN)_6].3H_2O$, p.a., ≥99.5%, Fluka), hexaammineruthenium (III) chloride (HAR, 98%, Aldrich) and 1,1´-ferrocenedimeyhanol (FDM, 98%, Aldrich).
Redox probe solutions of $[Fe(CN)_6]^{3-/4-}$ (HCF, 1:1), $[Ru(NH_3)_6]^{3+}$ (HAR) and FDM, at a concentration of 5 mmo L^{-1}, were prepared in 0.1 mo L^{-1} Na_2SO_4 electrolyte solution.
All aqueous solutions were prepared using water purified with a Milli-Q purification system (resistivity ≥18MΩ cm).

Instrumentation used in the electrochemical measurements

Electrochemical data were obtained using a computer-controlled potentiostat Autolab PGSTAT30 (Eco Chemie B.V., Utrecht, Netherlands) monitored by the NOVA 2.1.4 software package.
Gold screen-printed electrodes (AuSPEs) were purchased from Metrohm (DropSens, DRP-220AT). They include a gold disk-shaped (geometric area: 12.6 mm^2) working electrode, a silver pseudo-reference electrode and a gold counter electrode, all of them screen-printed on a ceramic substrate (3.3 cm×1.0 cm) and subjected to high-temperature curing. All potential values were referred to the screen-printed silver pseudo-reference electrode. The SPEs were connected to a switch box, also from DropSens (DRP-DSC), allowing their interface with the potentiostat. All experiments were carried out at room temperature (21 °C).

Instrumentation used in the eSPR measurements

The studies were conducted using a SPR Autolab ESPRIT (KEI bv, The Netherlands) controlled by KEI SPR Data Acquisition software (version 4.4). The instrument consists of two independent measurement channels and incorporates a robotic auto-sampler to inject all solutions used. Solutions were aspirated from any position of the 384 microwells

plate or from two available stock positions (for two different buffers). Together with the buffer flask solution, three different buffers can be added to the SPR cuvette using full-automated sequences. Solutions were injected into the measuring channels through two sharp needles that control the volume, frequency and mixing speed, for specified incubation time. In a typical experiment, 50 µL of sample solution were injected into the cuvette channels and the needles provided a continuous flow of solution over the SPR gold surface (pumping speed of 12.5 µL s^{-1}) by continuous aspiration-dispense cycles using a mix volume of 15 µL. To performed the electrochemical measurements, the pumping speed was reduced to 6 µL s^{-1} in order to minimize noise. The cuvette is connected to a pump to drain out the liquid from the measuring channels.

Prior to the SPR experiments, the flat glass disks coated with a thin gold film (≈50 nm, KEI bv, the Netherlands) were washed thoroughly with pure water and ethanol, followed by drying under N_2 flow. The SPR gold disks were then placed over the half-cylinder glass prism covered with a thin layer of refractive-index-matching oil and stand positioned inside the equipment in a Kretschmann optical configuration[1] to begin the measurements of the SPR reflected angle (in milidegrees, m°). Gallium-Arsenide (Ga-As) diode laser acted as a source with a fixed wavelength of 670 nm in combination with a scanning mirror to modulate the angle of incidence of plane polarized light beam on the SPR substrate.

The SPR Autolab ESPRIT allows to perform electrochemical measurements in one of the two channels controlled by an external potentiostat. Simultaneous electrochemical-optical measurements (eSPR) were carried out in the electrochemical cuvette cell coupled to a conventional three-electrode configuration system. The standard SPR gold chip was used as working electrode, an unshielded Pt bar was used as counter electrode and a Ag/AgCl (saturated KCl) wire as reference electrode. Electrochemical data were obtained using a computer-controlled potentiostat Autolab PGSTAT30 (Eco Chemie B.V., Utrecht, Netherlands) monitored by the NOVA 1.11 software package.

The temperature of the SPR cell was maintained constant and reproducible by using a Julabo F32-HE (Germany) water bath. All experiments were carried out at 25.0 °C, unless otherwise stated.

As a routine procedure, all buffer solutions were degassed before use to avoid any disturbance caused by air bubbles present at the SPR sensor surface. Furthermore, the following solutions: (1) 0.5% SDS aqueous solution, (2) 100 mM HCl, (3) ethanol, (4)

100 mM NaOH and finally (5) pure H_2O were passed through the SPR flow system (≈50 mL each) prior to the beginning of the measurements to keep it free of proteins[2].

Electrochemical measurements

Cyclic voltammetry (CV) was performed at a scan rate of 50 mV s^{-1}, unless otherwise stated, and square wave voltammetry (SWV) operated under the following conditions: step potential of 2 mV, pulse amplitude of 50 mV and a frequency of 25 Hz. Voltammograms were recorded in the potential range between -0.30 – 0.50 V for HCF and FDM, and between -0.60 – 0 V for HAR. The electrochemical conditions tested were: (1) single SWV measurement or (2) three CV cycles followed by SWV measurement.

Preparation of sensor surfaces

Before the eSPR studies, the flat glass SPR disks coated with a thin gold film (≈50 nm) were washed thoroughly with pure water and ethanol, followed by drying under N_2 flow. Prior to the electrochemical experiments, the AuSPEs were washed thoroughly with ethanol and acetone followed by electrochemical cleaning by cycling the electrode potential from 0 to 1.1 V at a rate of 100 mV s^{-1} in 0.1 mol L^{-1} sulfuric acid until the CV becomes stable (approximately 12 cycles). Finally, the electrodes were washed with ultrapure water. In order to perform the electrochemical measurements, the imprinted electrodes were coated with a 65 µL drop of the redox probe solution.

For the preparation of the modified AuSPEs, the AOT self-assembled monolayer was prepared by incubation of the working electrode with 18 mmol L^{-1} AOT aqueous solution (10 µL drop) overnight, at room temperature. The electrode was rinsed with water and dried under nitrogen flow. Furthermore, poly(3-aminophenol) and poly(thionine) films were deposited on AuSPEs by electropolymerizing 10 mmol L^{-1} of 3-aminophenol and 0.5 mmol L^{-1} of thionine, respectively, dissolved in PBS 0.1 mol L^{-1} at pH 7.4. Electropolymerization of 3-aminophenol was carried by collecting 3 cyclic voltammogram between -0.3 and 0.8 V at the scan rate of 100 mV s^{-1}. A similar procedure was employed in the electropolymerization of thionine, where 5 cyclic voltammograms were recorded between -0.6 and 0.7 V were recorded at the scan rate of 50 mV s^{-1}. The modified electrodes were thoroughly rinsed with pure water to wash away remains of the reactants, dried under a nitrogen flow and stored properly at room temperature.

Fig. S1

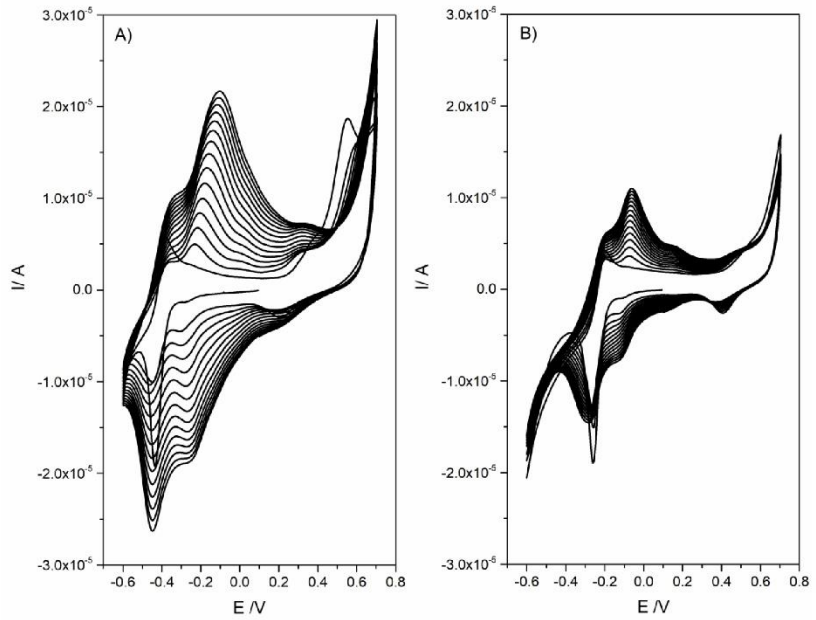

Fig. S1. CVs obtained for the electropolymerization of 1 mM thionine, dissolved in 0.1 M PBS pH 7.4, on the AuSPE, when (A) no measurements were performed prior to modification and (B) CV and SWV measurements, in the presence of 5 mM HCF redox probe, were performed at bare chip prior to modification.

Fig. S2

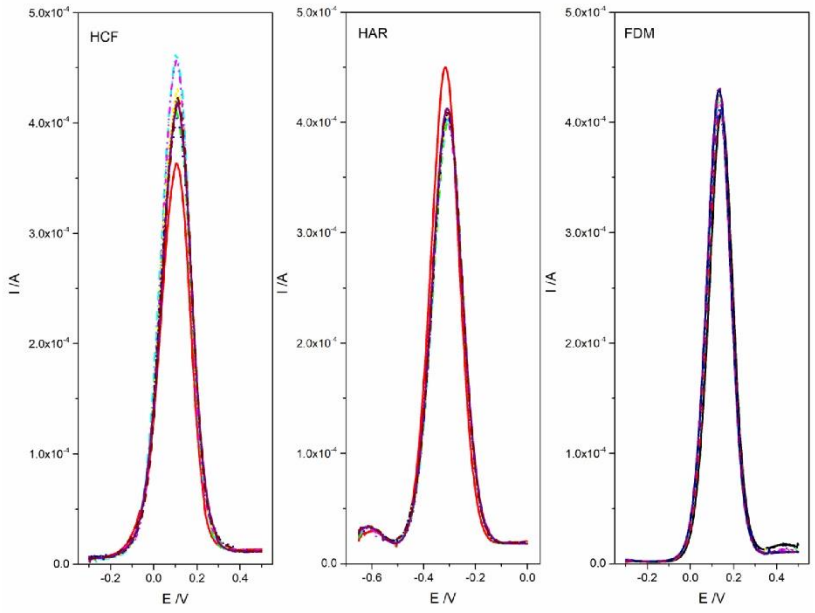

Fig. S2. SWV curves collected during the eSPR studies.

Fig. S3

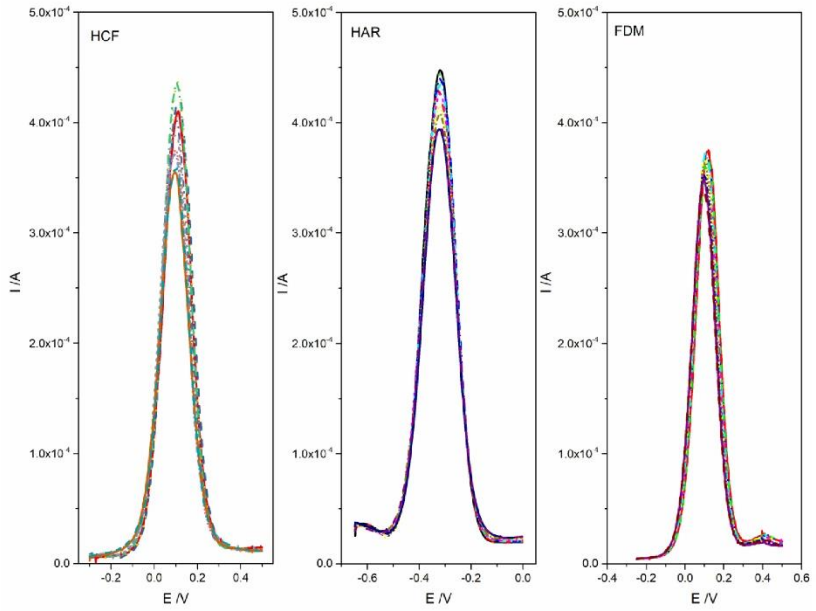

Fig. S3. SWV curves, collected after three CV cycles, during the eSPR studies.

Fig. S4

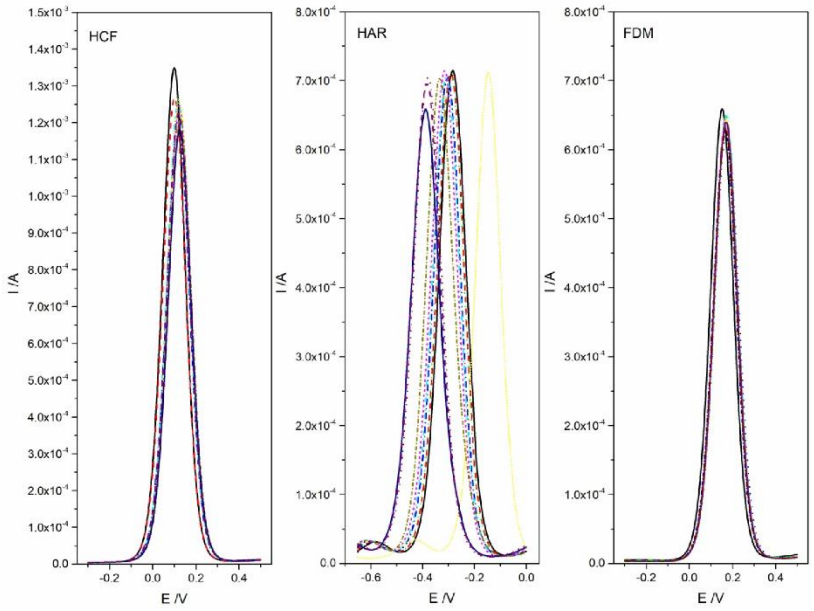

Fig. S4. SWV curves collected at the AuSPE.

Fig. S5

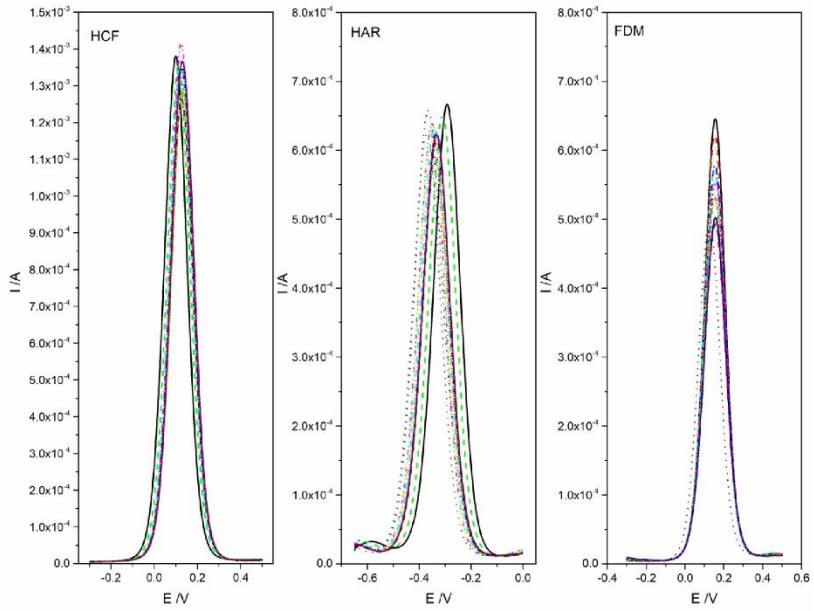

Fig. S5. SWV curves, collected after three CV cycles, at the AuSPE .

Fig. S6

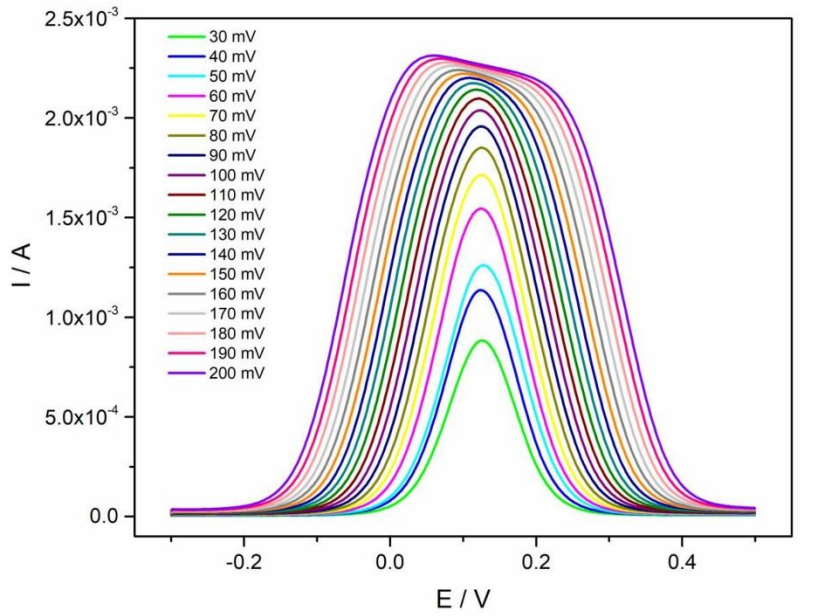

Fig. S6. SWV voltammograms obtained at bare AuSPE for different pulse amplitude values for the HCF redox probe.

Fig. S7

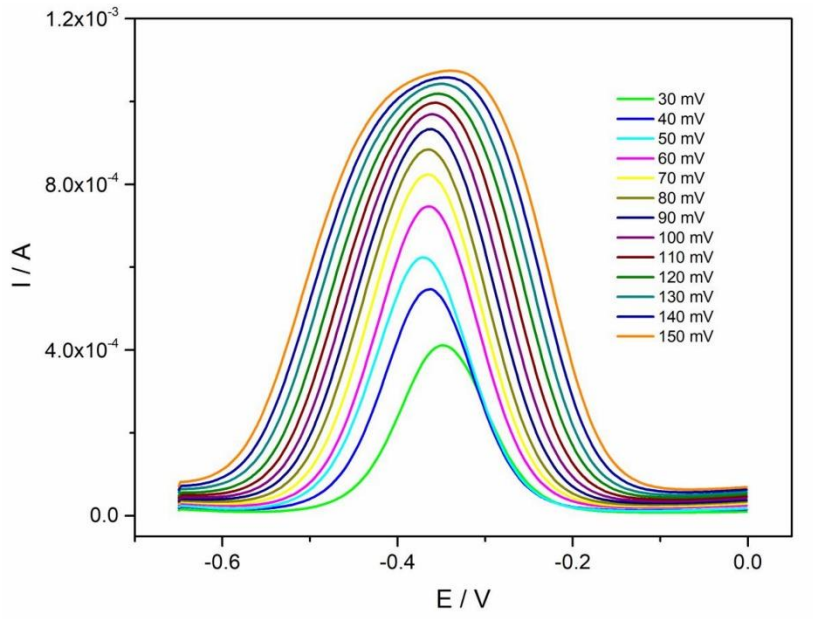

Fig. S7. SWV voltammograms obtained at bare AuSPE for different pulse amplitude values for the HAR redox probe.

Fig. S8

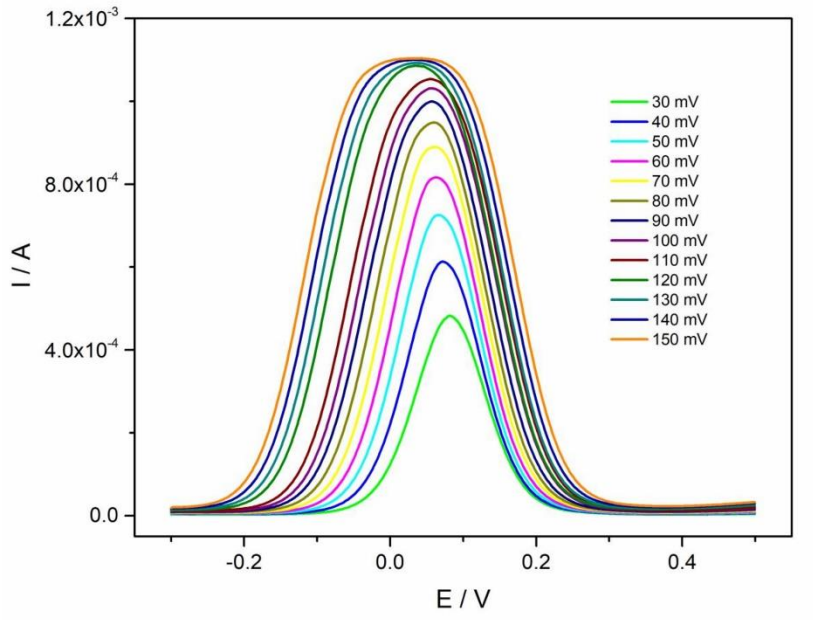

Fig. S8. SWV voltammograms obtained at bare AuSPE for different pulse amplitude values for the FDM redox probe.

Kinetic studies using polycrystalline gold electrode

Electrochemical kinetic studies with gold polycrystalline electrode (Metrohm ref: 6.1204.140; 2 mm diameter) were performed using a three-electrode cell. A SCE (3 M KCl) electrode was used as the reference electrode (Metrohm), and a large area helix-shape gold wire as the counter electrode, previously annealed for decontamination. The electrochemical cell placed in a Faraday cage in order to minimize the contribution of background noise to the analytical signal.

Prior to the measurements, the gold electrode was polished with a fine water based diamond polycrystalline suspension (1 μm, Buehler) on a microcloth pads (Buehler) followed by rinsing with pure water and brief cleaning in ultrasonic bath for about 10 min. The polished electrode was then electrochemically cleaned, by continuous cycling between 0 and +1.55 V, at 100 mV s^{-1}, in 0.5 M H_2SO_4 solution, in order to first oxidize and then reduce the gold surface. Finally, the electrode was rinsed with pure water and dried with nitrogen.

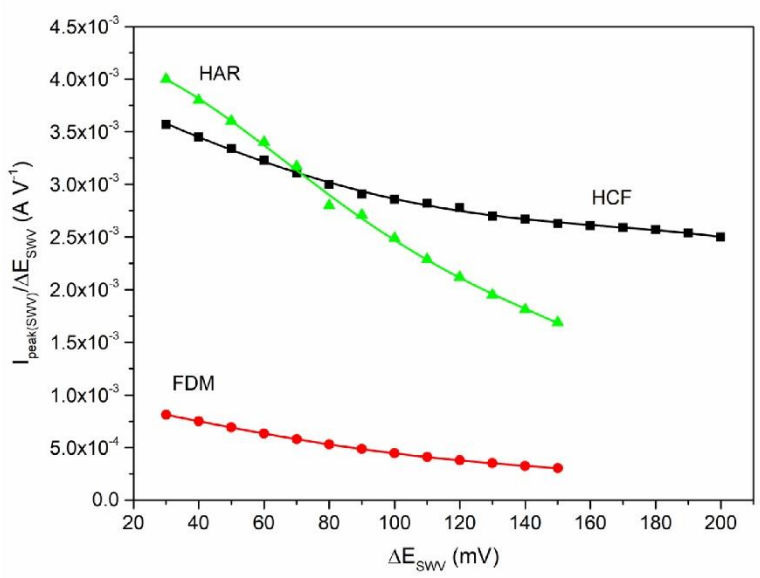

Fig. S9. Variation of the amplitude-normalized peak current in SWV ($I_{peak(SWV)}/\Delta E_{SWV}$) with the pulse amplitude (ΔE_{SWV}), obtained at the polycrystalline gold electrode surface, for the three redox probes studied.

References

[1] A. Kausaite, M. van Dijk, J. Castrop, A. Ramanaviciene, J. P. Baltrus, J. Acaite, A. Ramanavicius, *Biochem. Mol. Biol. Edu.* **2007**, *35*, 57-63.

[2] L. G. Carrascosa, S. Gómez-Montes, A. Aviñó, A. Nadal, M. Pla, R. Eritja, L. M. Lechuga, *Nucleic Acids Res.* **2012**, *40*, e56-e56; A. Aviñó, C. S. Huertas, L. M. Lechuga, R. Eritja, *Anal. Bioanal. Chem.* **2016**, *408*, 885-893.

Annex 2

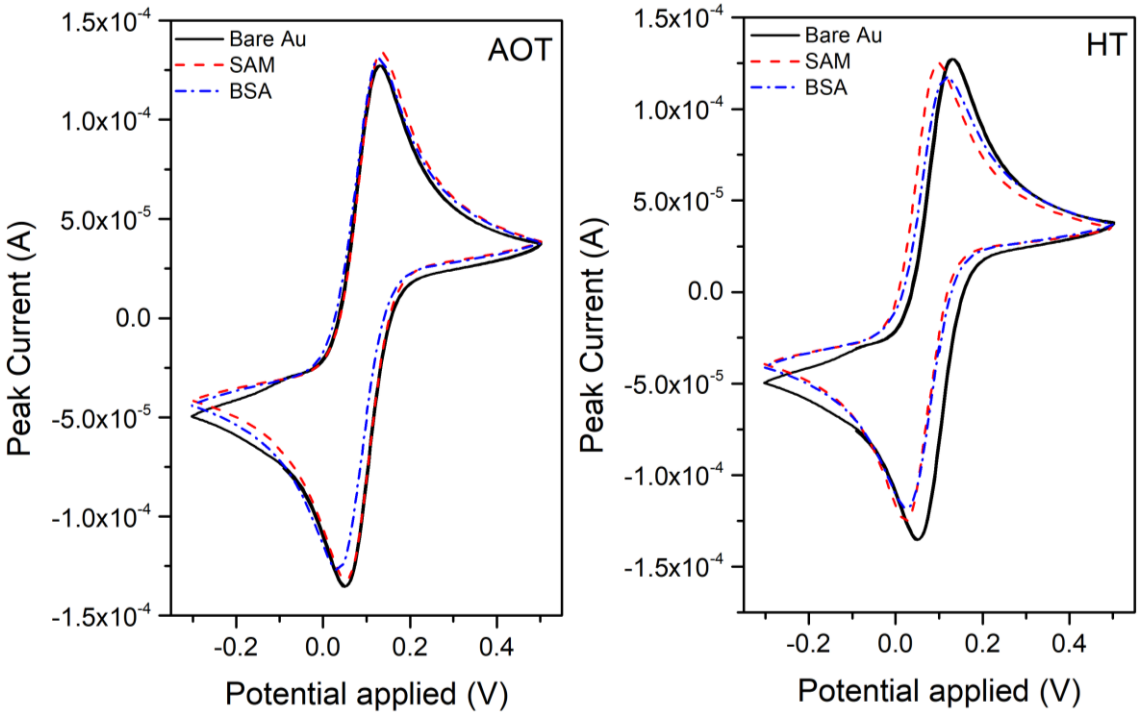

Figure A2.1 - Typical cyclic voltammograms obtained under the same experimental conditions.

Annex 3

Surface plasmon resonance (SPR) is an optical technique based on the measurement of the oscillation of the electron density caused by a p-polarized light, at the interface of two different media, namely a metal and a dielectric [55, 56]. Moreover, the sensitivity of the technique measurements makes it advantageous to perform biosensing studies with proteins [57].

The SPR measurements were conducted using a SPR Autolab ESPRIT (KEI bv, The Netherlands), show in Fig. A3.1. The complete SPR set-up, operation conditions and experimental details used for performing the SPR measurements are described in Supporting Information of the publication on Annex 1.

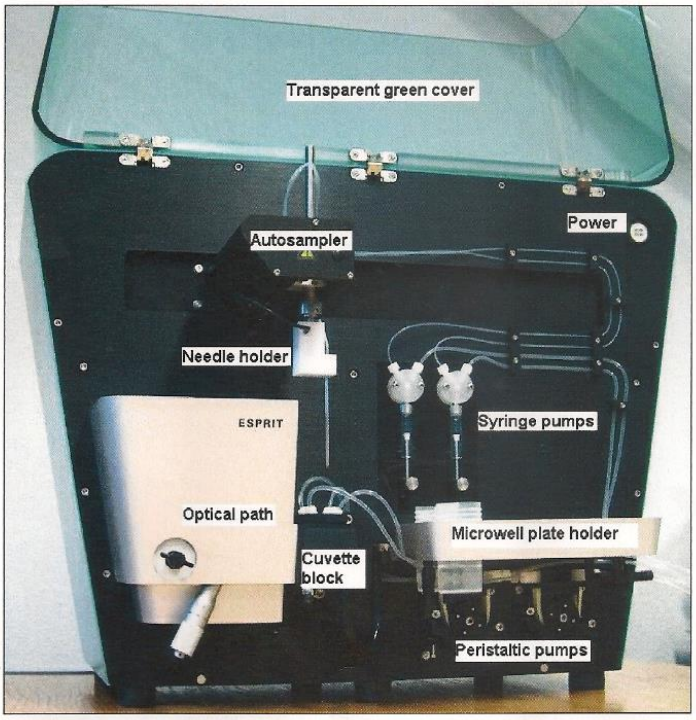

Figure A3.1 - SPR system used in this work.

The purpose of these experiments was to examine by SPR, in real-time, the adsorption kinetics of BSA on gold surfaces modified by alkyl thiols having different terminal functional groups: CH_3 (HT), NH_2 (AOT) and OH (MCH). SAMs of HT, AOT and MCH on gold SPR substrates were prepared by immersing the clean sensor surfaces into the thiols' solution overnight. Afterward, the modified chips were rinsed with pure water and dried under a stream of N_2.

Fig. A3.2 presents the experimental results obtained for the BSA adsorption on the SAM modified gold surfaces. The concentrations of BSA tested ranged from 1.0 to

500 µmol·L^{-1} aiming to determine the optimal template concentration used during immobilization step.

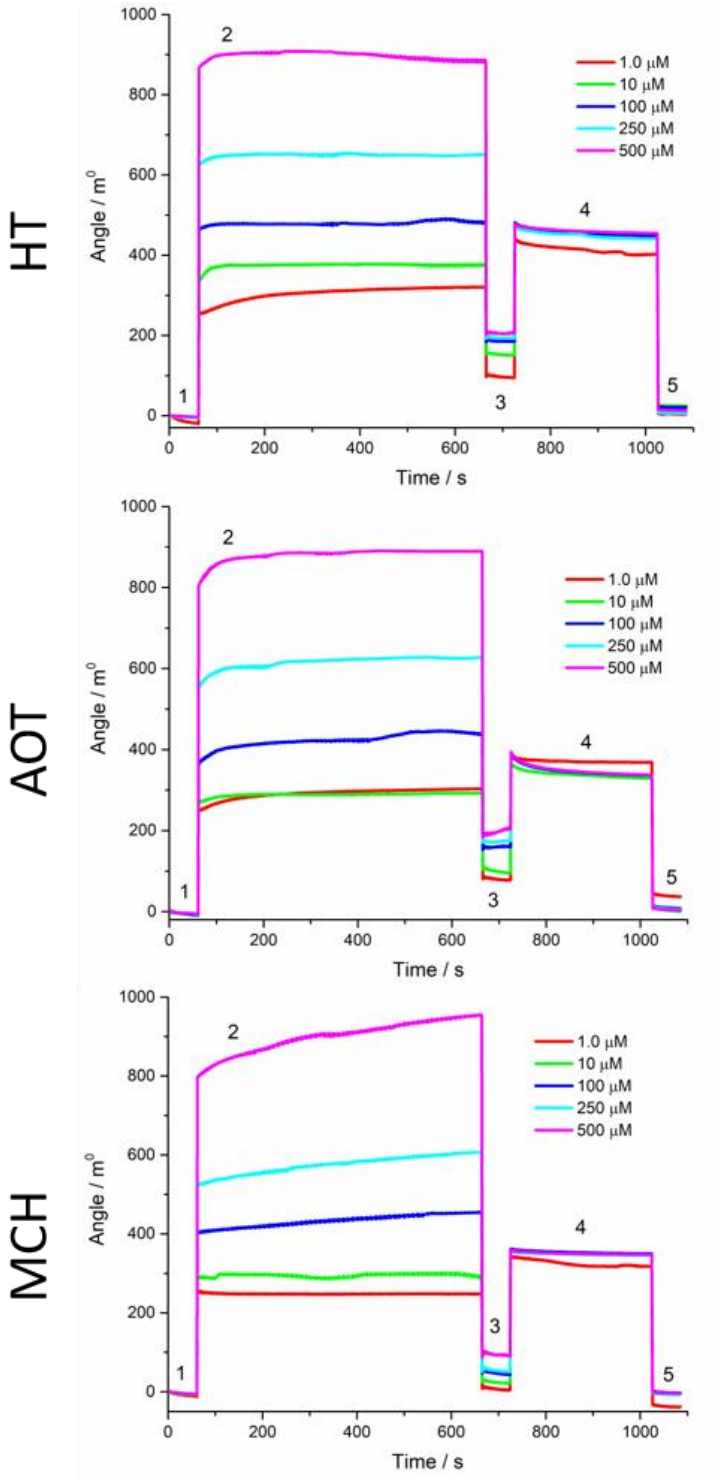

Figure A3.2 - Real-time SPR monitoring of the interaction between BSA and pre-formed SAMs of HT, AOT and MCH on SPR gold substrates. The concentration of BSA tested ranged from 1.0 to 500 µmol·L^{-1}. Line 1: baseline collected in 10 mM PBS, pH 7.4, for 60 s; Line 2: real-time monitoring of the BSA adsorption for 10 min; Line 3: surface wash with PBS for 60s (return to baseline); Line 4: BSA desorption after surface wash with 25 mmol·L^{-1} SDS solution, prepared in acetate buffer (pH 4.0), for 5 min; Line 5: wash with PBS for 60 s (return to baseline).

Based on the overall SPR angle variation due to BSA adsorption, after surface wash, for each concentration tested, a comparison of the amount of BSA adsorbed on each SAM surface is provided in Fig. A3.3.

As can be seen, the binding of BSA decreased in the following order:

CH_3 (HT) > NH2 (AOT) >> OH (MCH)

which is in agreement with results of literature reporting higher adsorption of BSA to hydrophobic surfaces compared with hydrophilic surfaces. The lowest amount of BSA attachment was measured on the neutral hydrophilic MCH surface due to the ability of OH groups to resist to protein adsorption. These results agree with the results reported in the literature revealing that BSA binding to thiol monolayers (having distinct terminal groups) is mainly controlled by hydrophobic interactions [58].

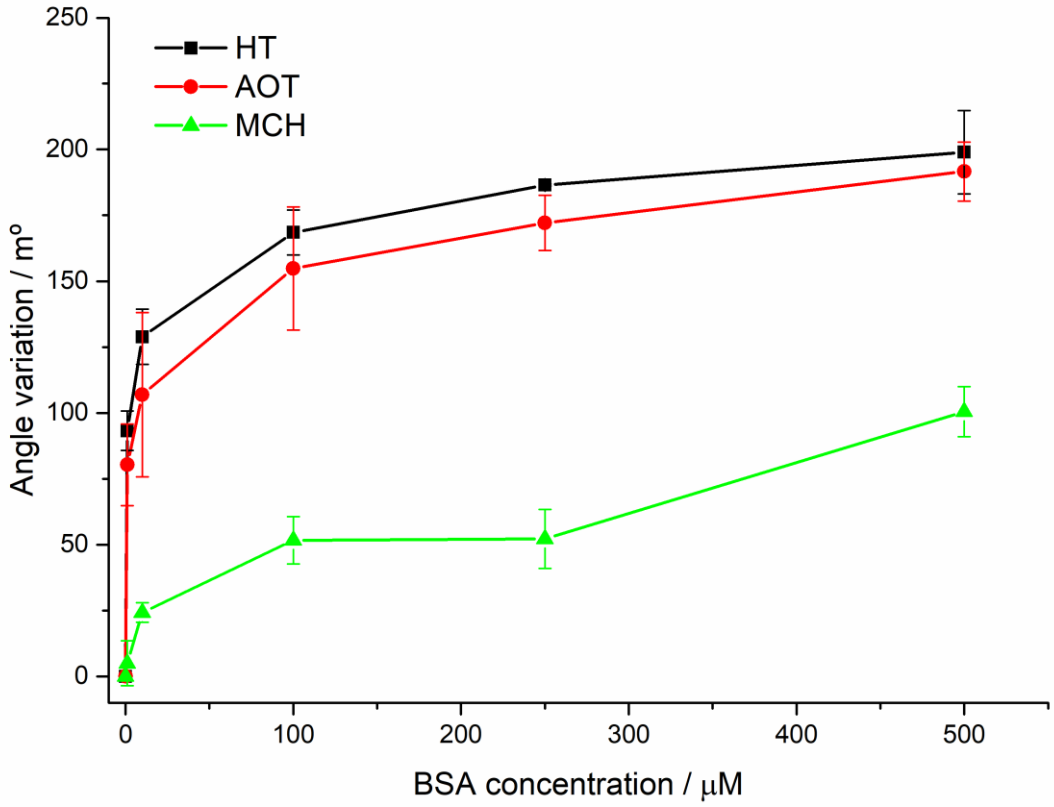

Figure A3.3 - Comparison of BSA adsorption on HT, AOT and MCH SAMs for each concentration tested. The error bars correspond to values collected from two independent experiments.

Annex 4

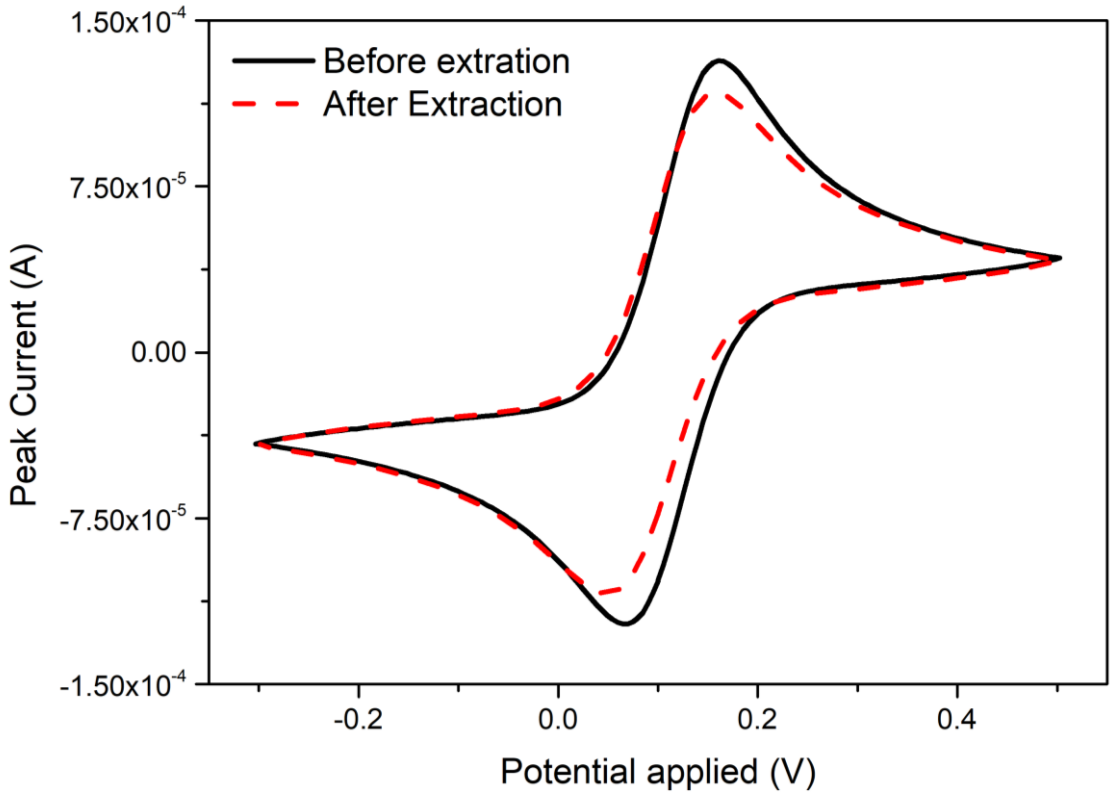

Figure A4.1 – Typical CVs voltammograms, obtained in the presence of a 5 mmol·L^{-1} redox probe solution, at the NIP surface (black) before and (red) after incubation with an acidic SDS solution overnight (extraction)

As can be seen, the SDS solution didn't affect the film stability, otherwise the peak current should increase. The observed decrease in peak current is probably related with remaining of SDS molecules adsorbed within the NIP film after surface wash.

Annex 5

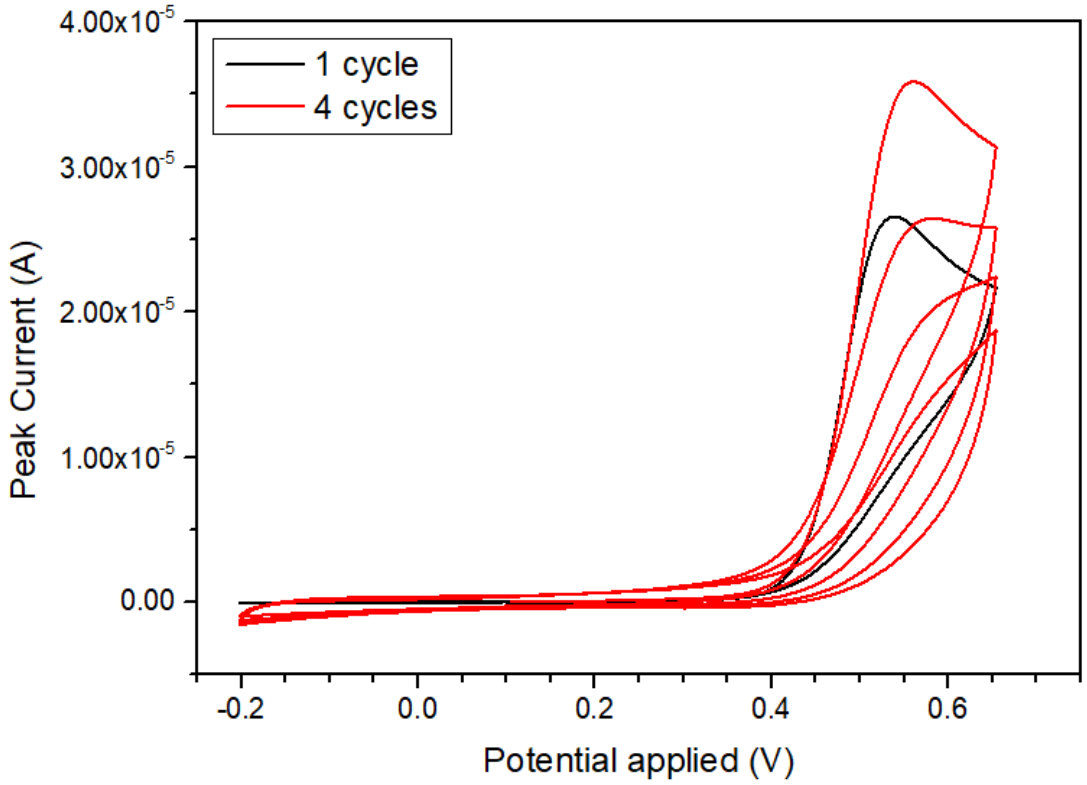

Figure A5.1 – Typical CV voltammograms obtained during the MIP electropolymerization using (black) one and (red) four CV cycles. Scan rate: 100 $mV \cdot s^{-1}$.

Annex 6

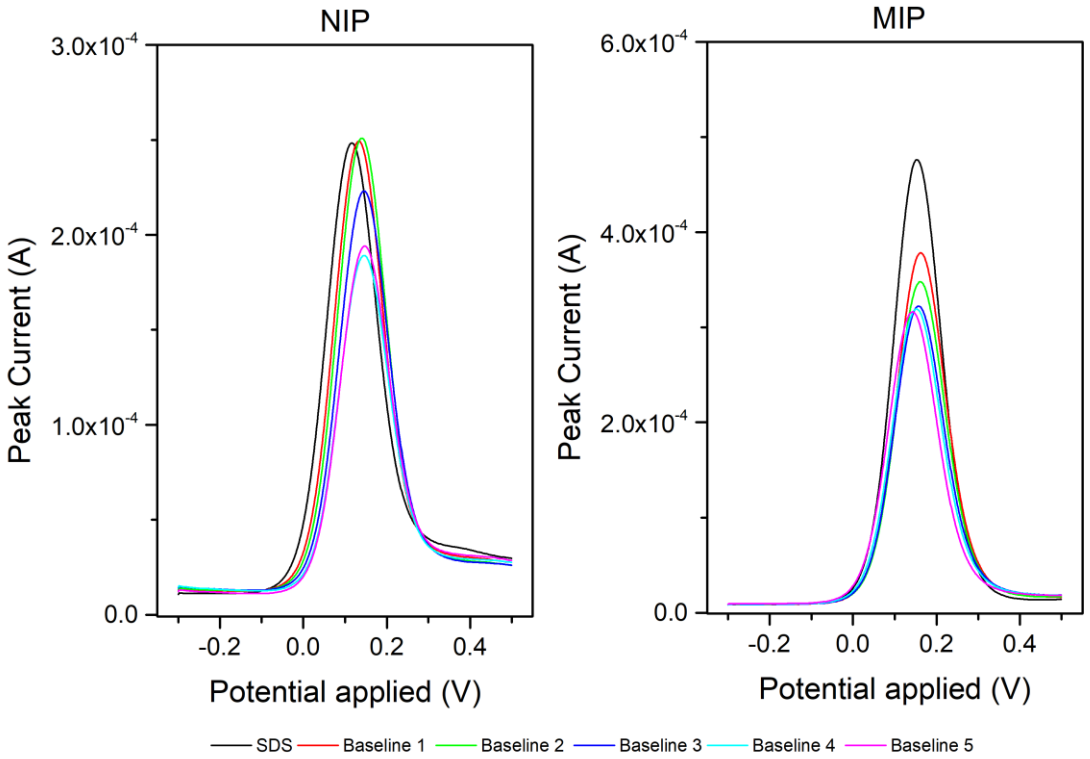

Figure A6.1 - Typical square wave voltammograms collected after repetitive incubations of the (left) NIP and (right) MIP surfaces, with PBS buffer